UNIVERSITY OF ZAGREB
**FACULTY OF ELECTRICAL ENGINEERING AND COMPUTING**

BACHEROL THESIS ASSIGMENT No.7063

# Analysis and design of wireless biomedical implant for patient monitoring

David Chuliá Mena

Zagreb, June 2020

**Table of Content**

# Introduction

The use of wireless communications in the field of biomedical technology is expanding the methods by which the patient can be diagnosed, monitored and, in specific situations, treated. However, the desired behavior of electromagnetic waves can be seriously affected when they interact with an inappropriate environment. The human body, characterized as a dielectric, is an obstacle to these communications, since it presents many losses due to the amount of water the body contains.

Among all the possible types of links in which the human body can intervene, the devices that must be inside the body are the most affected by the losses that the body presents. In these cases there is an intersection between safety, medical complications and electronic design complications: the size of the device.

In this document we will address the issues related to the wireless connection of an antenna located inside the human body and measure its efficiency, as well as other parameters that characterize wireless communication. Part of the work will be to scale the device to small sizes, establishing a compromise between the size of the antenna and the quality of the link. The device in question is an Arduino based prototype for monitoring human body temperature that should be located inside the human body. Although there are many electronic challenges to be addressed, in this thesis we will focus on the wireless part of the device.

To do this, we have made designs and simulations using the CST Studio Suite program. It has been essential to understand the physical fundamentals of antennas and, specifically, of free space dipoles in order to be able to interpret the results when they are inside a lossy material. We have focused on a high central frequency of 2.45 GHz to be able to use it with Bluetooth or Wifi. In addition, the bands of this technology support high data transmission rates.

Due to the complexity that supposes the electrical characterization of the human body, the models created in CST try to be simple models, as well as that of the encapsulation where our antenna and, theoretically, the rest of the electronic components are located. To determine how the different parameters of the antenna influence the radiation properties, like length, material, gap, we have had to keep some of them constant except the variables we are trying to deal with.

One of these variables, which is not a direct parameter of the electronic design, is the position of the antenna inside the body. This is a relevant measurement, since it will determine which is the thickness of the human body that has to cross the wave to reach the receiver that is outside the patient.

In general, this project does not aim to make a final product, but to characterize the variables and their effects in simple models of antennas and human bodies. A final product would not only address a much smaller electronic design than an Arduino, but digital modeling of the human body should be much more detailed. Different body tissues and organs have different permittivity and conductivity. This problem is not only found in digital simulations, but also in physical experimentation with dummies or phantoms, which, despite being a great option, are still an approximation materialized in an artificial construction without living tissue and under standards of average bodies with a certain height, weight, build...

The data simulated in the CST have been treated by numerical methods in Matlab in order to make better comparisons between the different measurements. Matlab offers us a

comfortable environment for dealing with large amounts of discrete data and vectors, which we have taken advantage of to extract conclusions by observing the different parameters of the transmission.

# Chapter 1: Biomedical Communications

**Types of biomedical communications**

Wearable and implantable biomedical technologies have grown rapidly in recent years. This type of communication can be used to track, record and monitor vital biological signals for medical purposes. However, this field can also be applied to sports, entertainment, smart houses or military purposes. This is thanks to the miniaturization of electronic devices, which, together with advances in communication and computing, allow us to carry increasingly smaller devices in our pockets or implanted in our bodies, making the implantation processes less invasive for the user.

The purpose of all this wireless communications technology in the body area network (WBAN) is the comfort of the user and the flexibility to perform specific activity for which it has been made. When it comes to in vivo medical implants, wireless communication is the most desirable for patient comfort and safety, as the use of cables can increase the risk of infection [1]. In addition, wireless communication always allows for longer distances to be covered. A classification of body-centric communications can be made [2].
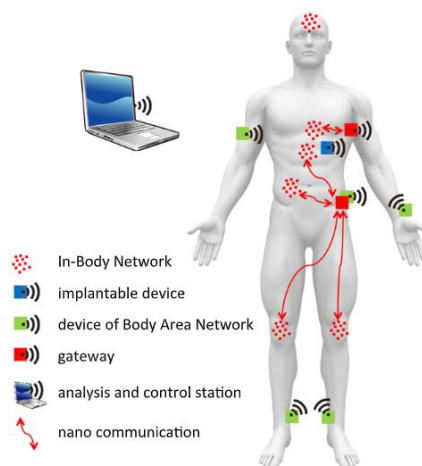


**Figure 1- Types of networks in WBAN [1]**

*Off-body to on-body communications:*

This type of communication refers to the transmission of information from an external device away from the body, such as a local reference point or access point, to a device on the body. This is what we know as a communication to a base station or broadcast station.

This type of communication is the most studied since it covers all the knowledge researched around mobile communications. Mobile phones are usually carried by the user at distances very close to the human body. Antennas must be able to orient their radiation pattern away from the body while having coverage in all directions.

The signal is exposed to most of the losses that any signal has in a usual environment: losses due to propagation in free space, refraction and multiple reflections, but the biggest obstacle is the body itself. The challenge is to execute and maintain good communication

independently of the relative position of the body with respect to the antenna: this implies any type of posture.

*On-body Communcations:*

This form of communication refers to the interconnections of devices that we wear on the body such as wearable computers, intelligent textiles or communications that take advantage of the currents in the user's body. One of the best known examples would be the smartwatches whose uses are usually focused on fitness tracking. On-body communications are capable of communicating with other devices that are also on the surface of the body, such as a smartwatch with a smartphone. Technologies such as Bluetooth or other similar standards are able to support high bitrates, which is interesting for the ability to send images.

In addition, the number of sensors they have can perform a telemetry of some biological signals such as heartrate, temperature, position via accelerometers. These sensors take advantage of the signals that can be captured on the surface of the body. However, there are a large number of biological parameters such as the levels of certain substances in the blood, chemical reactions, tissue movements or images that are not accessible from the outside. [3]

*In-body Communcations:*

It refers to communications executed by medical implants located inside the human body. The implants are placed in specific locations for use. The safety of the patient must be guaranteed, as the device must not interfere with the proper functioning of the body.

Once implanted, the device should not be removed again to replace the battery unless exceptionally necessary surgery is required. Although most in-body devices are implants, there are also other less developed technologies such as ingestible pills or injectables.

For example, Proteus Discover consists of a mobile application, a sensor and a pill that is able to transmit a signal from the stomach. Once the pill is swallowed, it is activated by a chemical reaction in the stomach and communicates with the sensor located in the torso. Microsensors in the pill are able to detect blood pressure, temperature, hear rate, and pH. [4]
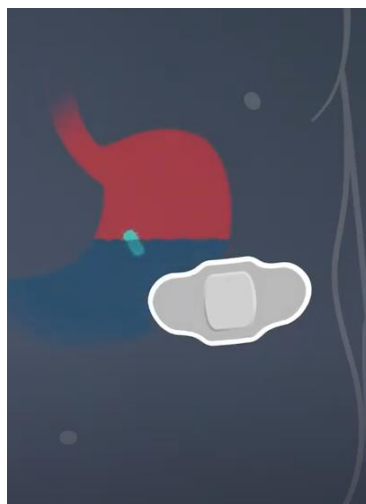


**Figure 2 -Proteus Discover Pill
(Source: Proteus Digital Health)**

We can say that the technological development of miniaturization and flexibility of sensors such as accelerometers, gyroscopes, temperature, etc. remains a challenge but, despite all

this, great advances and achievements have been made. However, the bottleneck appears in the aspects of communication, since fewer studies have been done on this subject. [2]

Antenna designs, the essential part of wireless communication, present great challenges in achieving a wide bandwidth. The main problem we find is the contradiction in needing a compact antenna, but at the same time we need it to be efficient: these two factors conflict.

First of all, we can think that using high frequencies solves the problem of size, since we increase the efficiency of small antennas. However, it is at the same time inefficient, since the attenuation presented by the human body and its tissues is very high. Secondly, to solve the previous point, it would be to think about increasing the power of the signal. But as we have mentioned, the implants have a battery which is not usually replaced and which, due to its size, does not have the capacity to supply as much energy. On the other hand, it should be noted that, feeding more power to a device that is, in itself, inefficient, only shortens the life of the battery.

As we can see, the design of this type of antenna is complex, as well as the choice of its power supply or frequency. Usually, for implantable devices, Planar Inverted-F Antennas (PIFAs) are used since they allow a good miniaturization. Helical antennas are used for ingestible devices as they allow a circular polarization and present an omnidirectional radio pattern. [1] Many frequency ranges are used for medical purposes, these ranges are determined by regulatory authorities and some of the bands are reserved for these purposes. The most commonly used bands for these purposes are the 403.5 MHz and 2.45 GHz bands, others like 867.5 MHz are also used, but with less frequent use and only available in Europe. In order to choose the optimal frequency, a trade-off has to be made between the advantages and disadvantages depending on the purpose of the device. Low frequencies are less affected in terms of propagation on conflicting channels. In our case, low frequencies have less difficulty in passing through body tissues, but require large electrical size antennas. In contrast, high frequencies allow us a higher data rate, which is preferable if our purpose requires the transmission of a large amount of information such as images or videos, but the body attenuation is very large and the losses are increased. As pointed out in Conor P. Conran's thesis in Antenna Designs for Wireless Medical Implants [10, 1], at frequencies of 3-5 GHz, 2 cm of biological tissue implies attenuation of between 20-30 dB.


**Precedents**

The design of implantable devices is a complex process. Technical problems must be solved by a compromise between the difficulties of electronics and medical guidelines. In spite of being a field of knowledge with a lot of potential and with a wide margin of improvement, we can affirm that medical implants are a reality. Nowadays a large number of patients are monitored and treated with implants inside the body, some of the most common being cardiac pacemakers or cochlear implants [5].

*Pacemakers:*

The trend in 2018 was that more than 1 million pacemakers are implanted per year. These devices help, through the generation of electrical impulses, to regulate the heart rhythm in patients who have their heart rate altered (the average heart rate of a healthy adult at rest is 72 beats per minute).

According to WHO (World Health Organization) data, diseases of the cardiovascular system, which consists of the heart and blood vessels, are the leading cause of death worldwide and are on the rise. The cardiovascular system is the transport system of our body.

It is responsible for delivering materials essential to the life of the cells and for carry away waste materials of the metabolism. All of this is transported by the blood due to the pumping of the heart.

As it has been possible to study with on-body monitoring, we have determined the behavior of the electrical signals that cause the heart cycle: the ventricles fill up during diastole and the ventricles contract during systole. This is due to the heart's natural pacemaker: the sinoatrial node. A regular electrical signal is sent to the top of the heart, where the atria are located, causing the contraction and pumping of blood into the ventricles (active filling, due to atrial systole). At this point the atrio-ventricular valves close and cause the first sound called S1. Then, the contraction of the ventricles and the difference in blood pressure causes the blood to be ejected into the arteries. This amount of blood is known as the stroke volume. When the pressure in the arteries is higher than the pressure in the ventricles, the blood does not return because the sigmoid valves close, causing the second S2 sound. The electrical signal travels from the sinatrial node to the atrioventricular node. It is this last node that produces a delay of 0.1s, which ensures atrial contraction before ventricular contraction. In case some phenomenon interrupts this activity, such as arrhythmias, it can affect the heart's ability to pump. In case some phenomenon interrupts this activity, such as arrhythmias, it can affect the heart's ability to pump.

The artificial pacemaker enables regular stimulation of the heart when the cells are not able to depolarize and fire action potentials at a regular rate. Until relatively recently, pacemakers provided non-programmable pacing along with questionable reliability and longevity. Today, advances have been remarkable: diagnostic capability through algorithms, adaptive pacing capability, data recording, and lithium-iodine batteries that extend longevity to 10 years.

Nowadays, the pulse generators are able to link up with the programmers through a wireless connection in a bidirectional way. The programmers are a telemetric device that connects the pacemaker to the clinician. In case the clinician wants to extract useful data or alter the patient's therapy, he or she can do it in order to optimize it. This real-time link can change the characteristics of the electric pulse generator in such things as amplitude, pulse duration or lead current among others [6] .
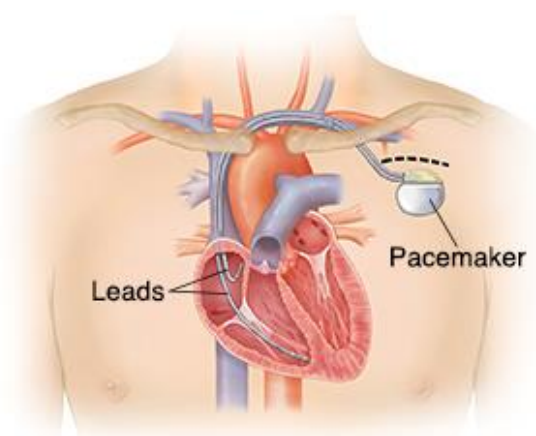


**Figure 3 -Pacemaker outline (Source: Mount Nittany Physician Group)**

For comfort, the latest advances in pacemaker communication are focused on the transmission of data to a server or in the cloud. This requires the programmer to be connected to the network. The improvements in the quality of life are multiple. The patient can travel with greater flexibility or be monitored from home. Likewise, the doctor can follow the pacemaker user's therapy without the user needing to go to a hospital facility.

*Cochlear implants*

Cochlear implants are devices divided into two parts, one internal and one external, which can qualitatively improve the hearing of the patient with severe sensorineural hearing loss. In order to understand how the implant works, it is useful to mention the functioning of the hearing system in general terms.

The hearing system is responsible for the mechanical capture and processing of sound waves. Internally, it converts the acoustic signal (mechanical wave) into nerve impulses and transmits them to the sensory centers of the brain. Finally, neural processing of coded information in the form of nerve impulses takes place. We can distinguish two regions of the auditory system. The first is the peripheral region, where sound stimuli retain their original character of mechanical waves until they are converted into electrochemical signals. The second is the central region, where signals are transformed into sensations. The central region also involves cognitive processes in which they are assigned a context in order to give meaning to the sound [7].

Cochlear implants can improve hearing in the face of malfunction of the receptor cells located in the cochlea, which are responsible for transforming mechanical waves into nerve signals. In the cochlea, sound passes through the basilar membrane, converting it into electrical impulses. The membrane filters the noise, the higher frequencies causing a higher vibration at the base of the cochlea and the lower frequencies at the top. This represents the distribution of frequency sensitivity in the cochlea. Its spiral shape causes it to start at a maximum of 20 KHz and go down to 20 Hz, thus showing a person's hearing range. This range gets smaller over the years and is often more pronounced in men than in women, especially for the higher frequencies.

Cochlear implants consist of two parts. The first external part picks up sounds from the outside with a microphone and processes them into a digital signal that is transmitted by a coil antenna into the hearing system [8]. It is at this point that the wireless link is essential to be able to transmit the signal inside without the need to have a hole and a cable running through it. If a cable is used, the patient will find difficult to live a normal life and there will be a great risk of infection and damage to the device.
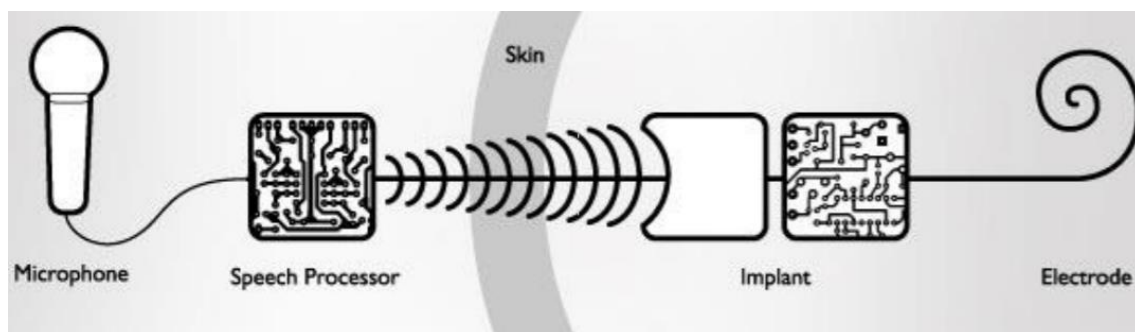


**Figure 4-Cochlear Implant Parts (Source: TIM subject FER, University of Zagreb)**

The second part of the device is an implanted receiver that sends the electrical signal to an electrode that is embedded in the cochlea. The electrode array is flexible enough to take on the spiral shape of the cochlea. The electrodes can stimulate many parts simultaneously. The distribution of the electrodes must be adjusted to the perception of the above-mentioned parts of the cochlea and to the frequencies that are sensitive. The distribution is logarithmic. The user's quality experience depends on several factors, but among them is the number of individual electrodes to stimulate the auditory nerves. Sounds are characterised by the timbre, which is not only a reference to whether it is higher or lower, but also to the texture of the sound. This kind of texture is the set of harmonics that a sound has, a quantity of frequencies that make us distinguish the sound of a piano from a violin even when they are playing the same note. Speech also has harmonics, a set of frequencies, it is not a pure sound. The more electrodes the cochlea possesses, the better the patient's experience will be and the more similarities it will have with the actual sound stimulus.

**Future uses**

As we have seen, implantable devices already exist today, but every step we take in seeking new solutions opens up even more challenges for us. In this section we will try to show how the biomedical technology sector continues to advance and there are many devices and prototypes that seek solutions to the diagnosis, treatment and monitoring of pathologies and biological signals.

For example, one developmental advance that will guide the pacemakers of the future is to make them leadless. Most often, experience complications are related to pacing leads. In addition, it is often preferable for patients to have more than one heart chamber excited for medical reasons. A recent prototype is a pacemaker whose parts act together as a leadless dual-chamber pacemaker system. For both parts to communicate they have to be able to have wireless communication with each other. Thus, the pacemaker in the right atrium (RA) sends a synchronization signal to the second pacemaker in the right ventricle. The result of the communication is optimal synchronization, establishing a delay that would naturally occur. Due to the short distance, the message is received almost instantly by the ventricular pacemaker in the same cycle as the systole-diastole heart. Therefore, the communication must be very efficient so that the pacemaker's lifetime will be long and not too much energy is spent on the wireless communication [9].
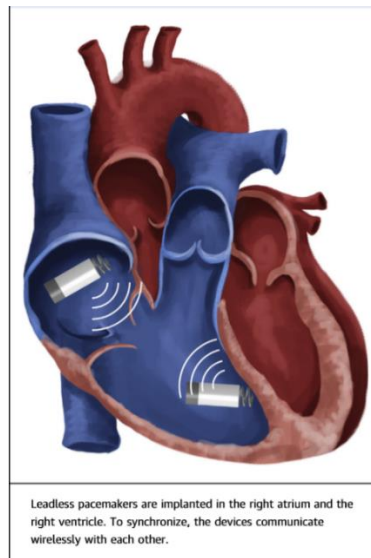
**Figure 4- Leadless Pacemaker (Source: Leadless Dual-Chamber Pacing [9])**

Another example of progress in research is the creation of an artificial retina. Retinal degeneration, such as makuladegeneration or retinitis pigmentosa, affects tens of millions of people worldwide. The artificial retinal aims to mimic the way the photoreceptors in the eye transform light into electrical impulses. This is done through an implant of electrodes that send out currents proportional to the light stimulus [10]. Thus, the goal is to replace degenerated photoreceptor cells with a microelectronic chip. However, we are far from recreating a reliable image of reality. The electrode arrays can only simulate a few pixels, which can give the patient basic information about the brightness or the presence of big objects, but are still images with very low resolution. Another research is also underway to change the architecture of the electrodes and instead of being a 2-dimensional array, to use a 3-dimensional one. It is expected that the 3-dimensional electrodes will be able to penetrate the inner limiting membrane and stimulate damaged retinal neurons more effectively than electrodes in a 2-dimensional arrangement [11].
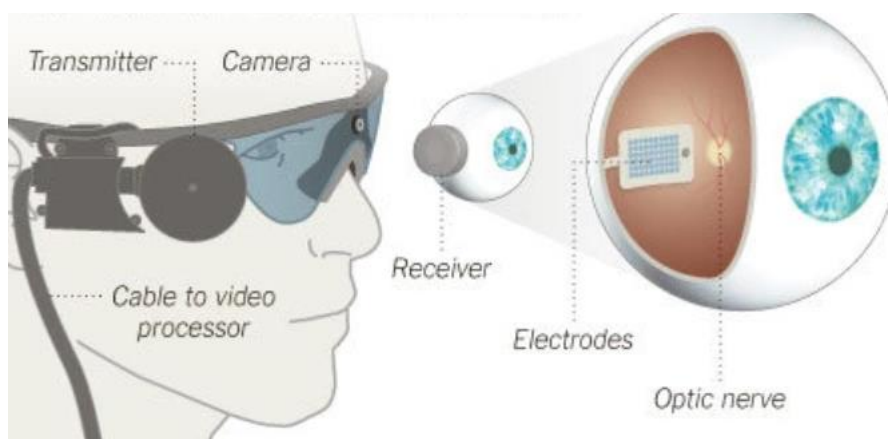


**Figure 5 -Artificial Retina Outline (Source: Second Sight Medical Products).**

12

There are many innovations in implant technology that are intended to be achieved. One of the most ambitious challenges is the transmission of images or videos via wireless links. Due to the nature of the images, the bandwidth required per frame is much greater than sending a few bytes of other biological signals. Wireless endoscopies are an example of a medical application where implantable antennas embedded in small devices play a crucial role. This would mean a change in the diagnosis of patients in the digestive system, which is traditionally wired. This wired method can be uncomfortable for the patient and can damage the digestive tract. The solution to this could come from the hand of a small pill that would be swallowed and transmit images in real time and without wires. However, for the correct diagnosis, high quality images are necessary, which would mean a relatively high bitrate and a higher energy consumption by an already limited battery. Therefore, the efficiency of the antennas plays a crucial role, since it allows to reduce the necessary transmitted power [1].

## Project Outline

In the project that concerns us, it aims to make a connection via Bluetooth between an Arduino device and a receiver. Of all the areas we can focus on in this brief description, the project has focused on the study of the transmitting antenna and all the parameters involved in establishing a radio link at 2.45 GHz. As we have pointed out on several occasions, the efficiency of an antenna is very important for medical implants when the conditions are appropriate for us in terms of size, losses and power supply.

The signal from the antenna must pass through a medium that, in electrical terms, is approximately the same as a human body. In other words, it is not a question of an end product, but rather of the study of signal propagation under unfavourable conditions. Due to obvious technical issues, lack of knowledge and resources, in-body to off-body simulation cannot be performed in vivo or with human tissues. A digital simulation with the CST program will be used for this purpose, although we will comment later on other options to test the correct performance.

The device is capable of measuring temperature through a sensor (theoretically body temperature) and knowing the orientation of the device through an accelerometer. However, we will not focus on the medical purpose of the device or the specific study of a diagnosis, or treatment. The Arduino we have used is the MK1010 model with a communication module from the NINA-W10 series, described as a basic module for IoT (Internet of things) applications. The module offers radio connection for Wi-fi 802.11b/g/n communications in 2.4 GHz ISM band and Bluetuooth v.4.2 (Bluetooth BR/EDR and Bluetooth low energy). As the specifications show, applications include low power sensor or medical devices among others. The internal antenna is a PIFA antenna specifically designed and optimized for the NINA form factor [12]. The VMA208 accelerometer is a smart low-power, three-axis accelerometer and the temperature sensor is the VMA320, which measures temperatures between -55°C to 125°C with an error of +/- 0.5°C.

**Figure 6 - Arduino MK Wifi 1010 (Source: Arduino Company).**

To study the size, materials and optimal position of the antenna, a dipole type antenna will be simulated in CST instead of the PIFA antenna of the communication module. The PIFA antenna is an inverted F-shaped type of antenna that has a top plate, similar to patch antennas. The dipole is chosen because it is a fundamental antenna whose architecture, operation and propagation are much simpler to study and therefore to simulate, interpret and process.

Another important aspect is the simulation of the antenna within some materials and offering a context in which the device can be placed. That is, on one hand, the theoretical device must be encapsulated so that the dipole does not short-circuit with the body and, on the other hand, the surrounding solid must be correctly characterized as a human body. The first thing is relatively simple, it is enough to encapsulate the antenna with air. However, simulating a solid so that its electrical properties resemble those of a real human body is much more complex. The number of different tissues and organs that make up the human body makes it difficult to create a very detailed solid. Moreover, extrapolating a model of a body to that of the entire population has its flaws: there is great variety between the anthropometry of people and their body composition due to various factors such as age, sex, diet...

With all the above aspects defined or, rather, approximated, the project focuses on seeing how the different parameters we can change from the dipole that affect the antenna's efficiency, the optimal frequency at it can radiate and the radiation pattern it generates. In addition, large amounts of numerical data can be processed in a better environment like Matlab using numerical methods. Matlab is often used as a programming environment in digital communications because of the flexibility it offers with vectors and arrays.

**Phantoms and test enviroments**

The measurements on which device radiation in human models is usually tested are often performed on phantoms. Phantoms are dummies that are intended to emulate a biological body. The materials and layers of the phantom are designed to simulate the characteristics of human tissue. The more plausible with reality, the better the interaction between the human body and electromagnetic fields can be studied.

Phantoms are usually used in medical diagnostic or treatment studies such as X-rays or MRIs. The use of phantoms is quickly justified; the application of methods that are in the early stages of development can be a danger for experimentation on living patients.

The use of phantoms is popular in the safe testing of human-related wireless communications, especially since the advent of mobile phones. Phantoms provide a safe and

stable environment for experimentation that would be difficult to do with humans. The manufacture of phantoms, to achieve the appropriate electrical properties, can be classified from two perspectives: the frequency in which it will be used and the type of tissue it is intended to simulate.

The classification of tissues can be divided into, first, tissues with a low water content such as bones or fat and, second, tissues with a high water content such as muscles, brain or skin. This second type, due to water, represents the highest loss and has the highest permittivity.

Liquid Phantoms

Liquid phantoms have been the oldest type of phantoms. This is due to its simplicity, as it is a container, usually made of fiberglass with low relative permittivity and conductivity. The container is filled with liquids that approximate the electrical characteristics of body tissues. However, the fixed composition of the liquid is not suitable for the whole range of the radio frequency spectrum, so it has to be adjusted to the desired range. This type of phantom is usually used for SAR (Specific Absorption Rate) measurements. SAR can be defined as the amount of energy that can be absorbed by a body through the influence of an electromagnetic field from an electronic device, usually a mobile phone, since it is the most popular device today, and we carry it most of the time and approach it to our head to talk.

The fiberglass shell may or may not have the shape of a human head or body with a hole to fill it with the liquid with the dielectric properties we want. The liquid may contain sugar to control the permittivity and salt to adjust the conductivity of the solution, among other possible substances. Although these phantoms allow us to study well the propagation of the internal part, it does not allow us to do the same on the surface of the body and does not take into account the heterogeneity of the human body.

*Solid-wet Phantom*

These types of phantoms have a gel texture that has been manufactured with the use of coagulants. This makes it easy to make a variety of molds, with many shapes for different types of body parts. Gel phantoms are suitable for simulating tissue with a high water content. As with liquid phantoms, the dielectric properties can be changed as the composition changes. However, these types of solids deteriorate over time due to loss of water or growth of fungi.

*Solid-dry Phantom*

Solid phantoms are made to preserve their shape over a long period of time. This is a good option for measuring SAR on the surface of bodies. In this case, the measurements are done by capturing the temperature of the phantom. In addition, depending on the phantom, it may have a heterogeneous inner part, like a real human body. However, due to some of the materials it is made of, such as ceramics, they are usually more expensive to manufacture than gels or liquids. Phantoms can also acquire various realistic natural postures. The extremities of these phantoms can be interchangeable. As with the previous phantoms, they must be manufactured with a human body dimension considered standard or average in order to extrapolate the results to the entire population.

*Numerical phantoms*

In order to find a solution to the heterogeneity of the human body and the amount of tissues it possesses, theoretical analysis on digital phantoms are proposed. This is possible thanks to the computational analysis through the technological advance in medical imaging and computational power. Phantoms are made up of a large number of small cells that, with increasing precision, describe human models and can simulate tens of different tissues [2].

*Test enivroments*

It is interesting to mention the use of these spaces that can be used for measurements with phantoms or other types of antenna. For example, the anechoic chambers is an installation used to test wave sources. The most characteristic features of this chamber are the covers of its walls: they can absorb, in acoustics, sound and absorb electromagnetic radiation when dealing with radiation in the radio frequency spectrum. The anechoic chamber is used to make more precise measurements and to isolate all kinds of noise coming from electromagnetic sources outside the studio. For this reason, the structure of the chamber must act as a Faraday's box. This makes the radiation isolated, from inside to outside the room and from outside to inside. The chamber's function, in addition to isolating from unwanted sources, also has another: it minimises reflections, emulating free space, but without the need to move a complete laboratory to an unobstructed location. The attenuation of reflections is produced by the material of the walls and their structure. Almost all anechoic chambers usually have absorbent ferrite tiles on the walls that are used together with long absorbent pyramids (porous foam, fibreglass...). Flexible carbon-impregnated foam pyramids can attenuate the radio signal by 45 dB. The anechoic chambers must be larger than the resulting useful space, as the thickness of the walls and the absorbent materials reduce it. For some measurements this is especially important, as several meters are required between the receiver and the transmitter, for example in the case of a connection between a phantom holding a mobile phone near the head and the source.



**Figure 7 -Solid-dry Phantom in an anechoic chamber (Source: Bloomberg)**

Another type of environment is the Open Area Test Sites, these environments are wide environments where the distances between the links are several meters and are made in open areas with no other nearby sources and little electromagnetic noise in the environment and in places free of nearby metallic objects such as fences, power cables. This kind of places are much cheaper than anechoic chambers.

Finally, at certain moments, when the intention in the test is to have an environment with many reflections and see how the link behaves, we can count on the reverberant chambers. These chambers have walls with very little loss and can act as resonators. The size of these rooms depends on the frequency you want to test. For frequencies of the order of gigahertz, very small chambers, such as 0.25 cubic meters, are enough [13].

# Chapter 2: Physical Basics of Wireless Communications from a Small Antenna Inside the Body

**Efficiency**

One of the parameters that we are most interested in when creating our wireless connection using antennas is the efficiency parameter. The efficiency is the ratio between the radiated power and the power delivered to the antenna. This means that not all the power delivered from the generator is radiated, but part of it will be dissipated and reflected. In order to understand the relation that it has with the impedance of the antennas it is necessary to make a brief explanation.

All antennas have an impedance on their terminals. This is the ratio between the input voltage and the input current. This impedance is a complex number, whose real part is the resistance and the imaginary part is the reactance. The reactance, ideally should have a null value, zero. If the reactance is equal to zero, we can say that we are talking about a resonant antenna in a certain frequency or a range of frequencies.

$$Z_a = R(w) + jX(w) \tag{1}$$

$$Z_a = R_r(w) + R_{ohm}(w) + jX(w) \tag{2}$$

The real part of the antenna impedance is the sum of the Radiation Resistance and the Loss Resistance. The Loss Resistance refers to the non-radiated power, and this resistance will increase if it is near a body with high absorption such as a human body. In most antennas $R_\Omega$ (Loss Resistance) $<< R_r$ (Radiation Resistance), however, the loss resistance is usually more substantial and critical on electrically small antennas (compared to wavelength).

On the other hand, the Radiation Resistance represents the energy that is radiated into free space. The power that would dissipate this theoretical resistance in a circuit would be the power that would be radiated by the antenna. Small antennas are usually less efficient, which means that their radiation resistance is lower. This is why effective miniaturization techniques for this type of device are important.

With the defined impedances, it is always important to transmit the maximum possible power to the antenna. This means to have the antenna matched. According to the maximum transfer theorem, the generator impedance should be equal to the antenna impedance. Since the generator impedance is usually real, the antenna impedance should also be real and should have as little imaginary part as possible.

$$Z_g = Z^*_a \tag{3}$$

$$P_a = \frac{V_g^2 \cdot Z_a}{(Z_a + Z_g)^2} \tag{4}$$

According to the above formula, it is not convenient to have a very small $Z_a$ because the power of the antenna would be low. On the other hand, it should not be too high with respect to $Z_g$, since the power would be almost zero. In the following graph you can see how the power of the antenna varies depending on how many times $Z_a$ is higher than $Z_g$ (taking real values). As we can see, taking arbitrary and constant values of $Z_g$ =50 ohms and V= 24 volts, the maximum power point is found just when $Z_a = Z_g$.
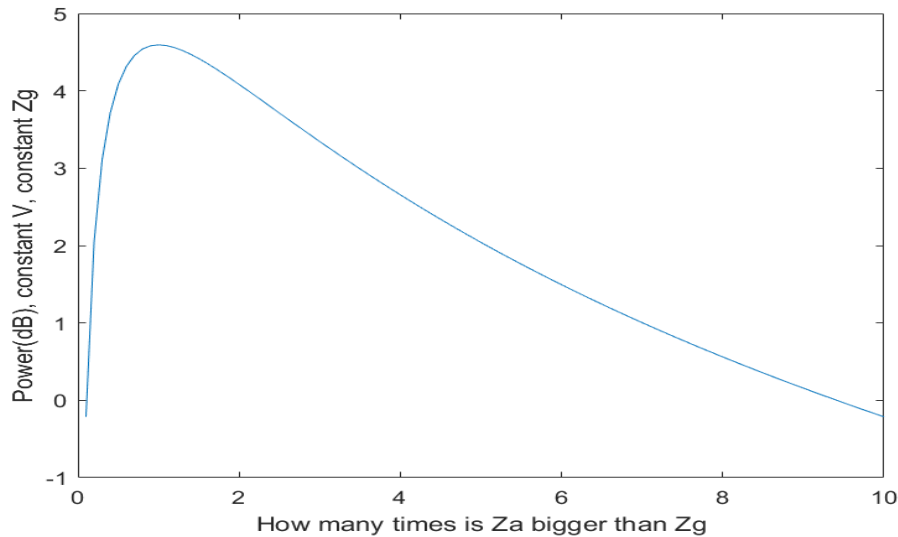


**Figure 8- Graphical representation of Maximum Transer Theorem**

In the case of matching, half of the power supplied from the generator is dissipated in the generator resistor and the other half is delivered to the antenna. This means that if we replace the antenna with the radiation resistor it would dissipate the same amount of power as the antenna would radiate under the same circumstances.

At low frequencies (with large wavelength) transmission lines are usually not a big problem. But at high frequencies where wavelength is electrically comparable to the size of the line, there are problems with cable impedance matching. Usually the transmitter can be placed far away from the antenna by placing a waveguide or transmission line in between. The participation of these elements must be taken into account to have a good matching since their length, attenuation and characteristic impedance are important aspects for a good working. According to the transmission line theory, if the antenna is not matched, some of the incident power from the generator will be reflected back to itself. In cases of unwanted high reflections, the return power could damage the amplification stages of the generator.

If we look at the input impedance equation, we can see that with a $Z_a = Z_0$, then, $Z_{in} = Z_a = Z_0$ regardless of the line length.

$$Z_{in} = Z_0 \frac{Z_a + jZ_0 \cdot \tan(\beta l)}{Z_0 + jZ_a \cdot \tan(\beta l)} \tag{5}$$

The reflection parameter $\rho$, which is between values [-1 and 1], is based on the following formula:

$$\rho = \frac{Z_a - Z_0}{Z_a + Z_0} \tag{6}$$

And the standing wave ratio:

$$SWR = \frac{1 + |\rho|}{1 - |\rho|} \tag{7}$$

This means:

Perfect match $\rho = 0$ and $SWR = 1$ (cause $Z_a = Z_0$)

Total mismatch $|\rho| = 1$ and $SWR = \infty$ (cause $Z_a = 0$ or $Z_0 = 0$)

With all this in mind, we can understand how the efficiency of the antenna is closely related to the impedance of the antenna and emphasize the importance of optimal radiation resistance. Following the definition of the radiation efficiency, we can derive its equivalent calculation as a function of the two resistive parts of the antenna impedance: the loss resistance and the radiation resistance. [15]

$$\eta_r = \frac{P_{rad}}{P_{in}} = \frac{P_{rad}}{P_{rad} + P_{ohm}} = \frac{I^2 \cdot R_{rad}}{I^2 \cdot (P_{rad} + P_{ohm})} = \frac{R_{rad}}{R_{rad} + R_{ohm}} \tag{8}$$

It should be remembered that ideally $Z_a = Z_0$ (if the transmission line is a relevant factor) and $Z_a$ in that case is a real number, with $R_r$ (radiation resistance) as the only component. In the following graph we can see how the efficiency in dB varies (from 0 to 1 in linear) depending on how many times the loss resistance is higher than the $R_r$. We can observe how the efficiency decreases as the loss resistance increases with respect to the radiation resistance.
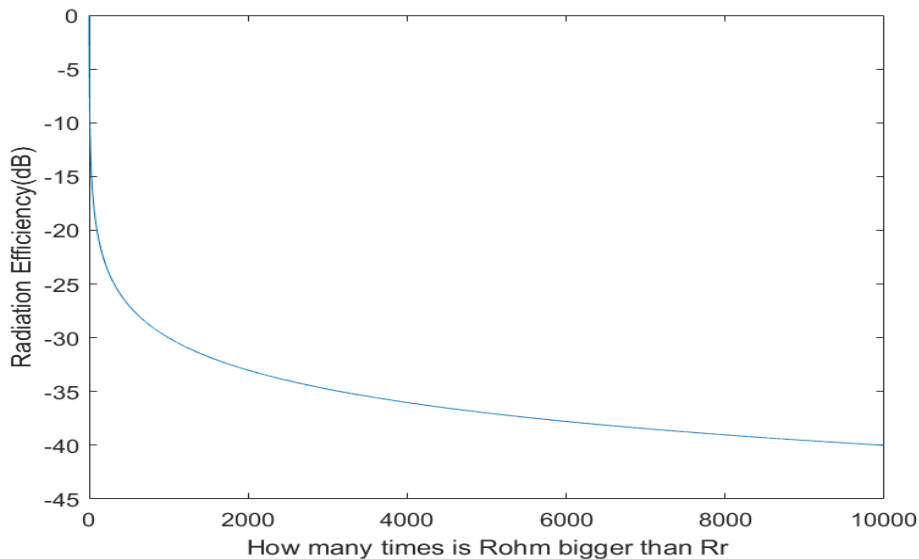


**Figure 9- Graphical representation of drop in efficiency as function of Rohm's (losses) increase**

The radiation efficiency of antennas can fall drastically due to the presence of objects and other factors such as parts of the human body. Due to the complexity of the calculation, the use of simulators becomes almost indispensable to make a systematic analysis. This type of electromagnetic studies are common with mobile phones in the presence of body parts such as the head or arms that can interfere with the efficiency of the antenna. That is why, for complex environments, the use of simulators is necessary.

If a generator delivers 1W of power to the antenna, the antenna will radiate the same amount of power if it has an efficiency of 1 (100%) in the best case (the antenna does not amplify the signal). Another way to define efficiency is the relationship between gain and directivity. The directivity would refer to the power radiated by the antenna while the gain definition would refer to the power delivered to the antenna. The difference between the two powers is the power dissipated by the antenna due to ohmic losses.

Another problem with electrically small or miniature antennas is their low radiation efficiency. Decreasing the length of the antenna means that the radiation resistance decays quadratically while the loss resistance decays linearly. For that reason it happens that the shorter a dipole is, the more inefficient it becomes. A small antenna is never interesting for transmission because we do not want most of the power to be dissipated as heat. [15]

However, there are cases where small antennas are practical because of their size depending on their purpose. Miniaturization methods have to be employed to improve efficiency, bandwidth and to reduce reactive impedance. The most common in practice is to use antennas that are between $1/8 \lambda$ and $\lambda$.


**Risk and damages to the human body**

Medical implants have a clear medical purpose to diagnose, monitor or treat the patient. Since they are devices embedded inside the human body, there are many factors that must be taken into account to ensure that they not only function properly, but also do not cause a risk to the patient's health. This involves issues such as rejection of the device by the body (such as the generation of granulomas, inflammations), tears or physical damage due to the shape and dimensions of the device or the materials that compose it which may be toxic. However, with regard to wireless communications, some fears have also arisen about possible health effects.

Today, in a world of growing communication systems and high spread of any kind of information, whether rigorous or not, opinions are being voiced against proximity radio frequency communications, skeptical about their innocuousness for human health. As with new technologies that work at a higher frequencies such as 5G, some people are alarmed, this fear has also spread with the proximity of the source transmitting radiation or continuous exposure over long periods of time (the Wifi router or mobile phones).It is to be expected that implants with antennas can cover all these fears, causing part of the population to reject them as being harmful to health.

There is a consensus in the vast majority of the scientific community on the health effect of RF communications: there is currently no scientific evidence of harmful effects on the body due to normal exposure (in terms of time and power) in the non-ionising spectrum. It is

known that RF radiation (reaching 300GHz) has the ability to warm a body, however, the power at which the signal is emitted is so low that it has no relevant effect and the higher the frequency, the less penetrating power it has.

However, there are some scientific articles that show the damage of radiofrequency in the human body. But the papers that claim this have a questionable methodology. In the scientific method it is important that the experiment is rigorous and replicable, so that anyone else can arrive at the same results, it is important. So how do we know if those articles are valid or not? The rigour of these papers can be judged by the impact they have. The impact would measure the final assessment of the work. The good scientific paper would open more pathways for research, stimulate other scientists and should be referenced in the new papers it has inspired. The mention thus becomes a form of validity by the scientific community, thus establishing a criterion of usefulness. The impact is a considerable value but there are other factors that show the quality of the article. [16]

That said, a large sample and correct isolation of the study variable are needed to avoid bias. The duration of epidemiological studies on health effects can be years or decades. Incomplete methodology may lead to false positives or a non-objective reading of the results where correlation does not imply causality. This is even more evident with the cancer-RF radiation relationship, without taking into account aspects such as food, contamination, or genetics. Other experiments with rats are also criticised from various points of view: daily exposure to rats may be longer and higher than that to which a human is exposed, control rats may be healthier than the control rats from previous studies, the rat population may be a small number.

Many rigorous studies remain to be done and the scientific community should not stop investigating the possible effects of non-ionising radiation under non-thermal conditions. However, one must be aware of the current evidence and the community consensus.

# Chapter 3: Simulations in CST Suite Studio

**Dipole modeling and results**

The first decision we have to make in the simulation is the size of the antenna. The length of the antenna, specifically, is a relevant parameter, since it will determine its efficiency and the frequency range in which it will be useful to us.

Our goal is that within that frequency range in which the antenna is resonant, it can radiate at a frequency of 2.45GHz. For this we have simulated several dipoles made of copper with the following specifications:

$$central\ frequency = 2.45GHz,$$

$$\lambda = 122.4490\ mm;$$

$$r_{copper\ dipole} = 1mm;$$

$$Gap = 5\ mm;$$
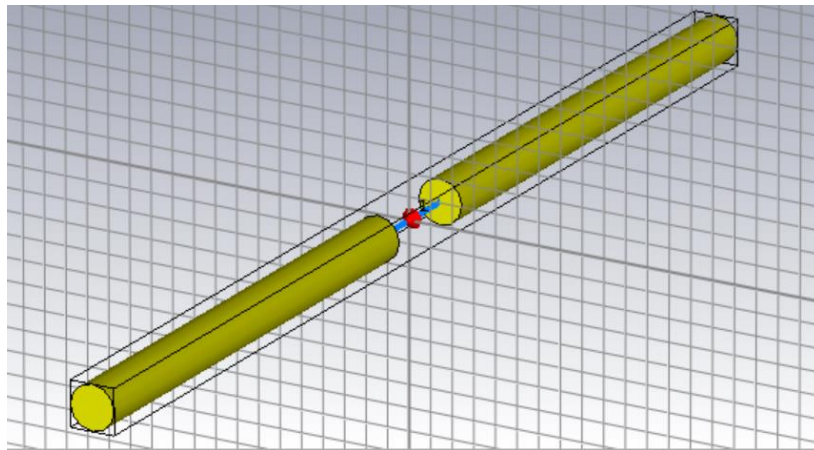


Figure 10- Dipole modeling in CST

In the following graphic, using Matlab, we can see how the values of the $S_{11}$ parameters are for all the lengths that have been simulated.

$$Given\ lengths\ of\ dipole\ l = \ \lambda, \lambda/2\ and\ \lambda/4$$

We can see how, after the CST simulations, we observe a clear trend: the shorter the dipole, the better it works for higher frequencies. The higher the frequency, the shorter the wavelength. Thus, for high frequencies, small antennas (in absolute terms) can be electrically long and therefore efficient antennas. For our 2.45GHz case. The most efficient dipole

approaches lambda/2 (61.2245 mm), although it would need to be adjusted and shorter.
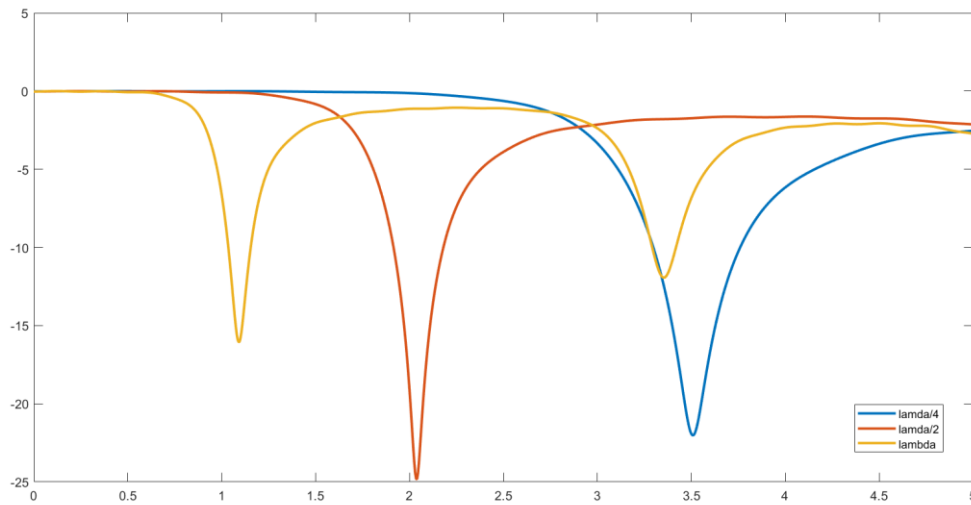


**Figure 11- s11 parameter for dipole with length lambda, lambda half and lambda quarter. Gap=5mm**

In this case we have changed the Gap between the copper cylinder , now is double (10mm respect the previous 5 mm). One of the clearest differences we see is the frequency at which the parameter $S_{11}$ is centered (on its minimum value in dBs close to 0 in linear).  In the case of the gap 10 mm it occurs at lower frequencies than when the gap was 5 mm. This change ocurrs because the inductance and capacitance is dependent on the length of the antenna, thickness and its structure (e.g. copper cylinders is made of). That means that the resonant frequency (where the impedance of the antenna is purely real) changes depending the reactance values, as well as RLC circuits.
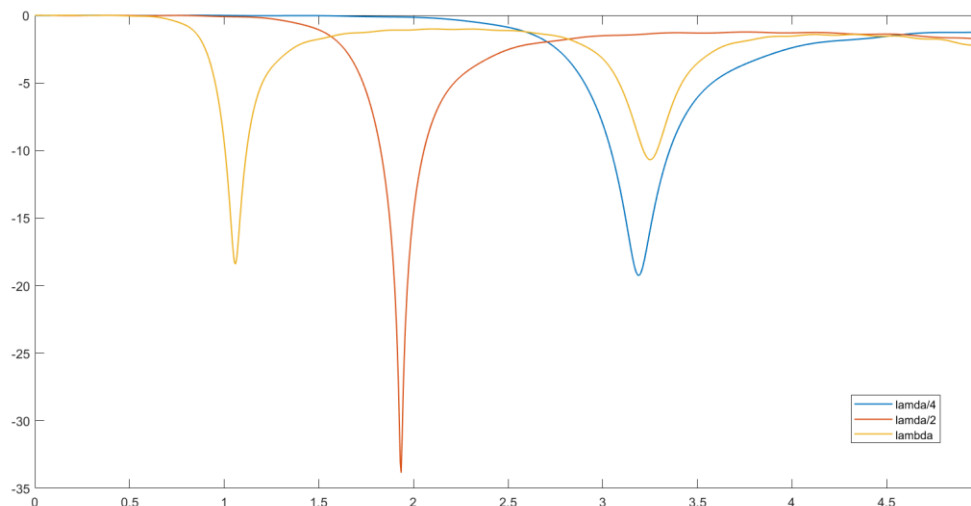


**Figure 12- s11 parameter of dipole with length lamda, lamda half and lambda quarter. Gap=10 mm**

However, although it is interesting to know the behaviour of the parameter $S_{11}$ as a function of the length and other values, for the following simulations the antenna model has been standardized to an ideal wire of lambda/4 length for the following reasons:

-We isolated the study parameter: the efficiency as a function of the position.

-We fixed other parameters such as  the material, the gap, or the dipole radius.

-It requires less computational time to complete each simulation.

This is the way to justify the use of an ideal cable. The way to justify its length to lambda/4 is a question of practicality in the environment. We must not forget that we are not only trying to find an efficient antenna but also a small one. In this case the length is a critical parameter. It is necessary to select an electrically and physically smaller antenna.

## Microstrip

Apart from the dipole, we have been able to simulate in the CST a microstrip antenna with the following characteristics:

| | Length (mm) | Width (mm) | Thickness (mm) | Radius connector (mm) | |
|---|---|---|---|---|---|
| **Ground** | 70 | 32 | 0.2 | **Pin** | 0.45 |
| **Patch** | 27.8 | 32 | 0.2 | **Teflon** | 2.05 |
| **Substrate** | 70 | 32 | 4 | **Coverage** | 3.175 |
| **Plate** | 32 | 4.4 | 0.2 | | |

**Table 1-Sizes of the microstrip antenna**
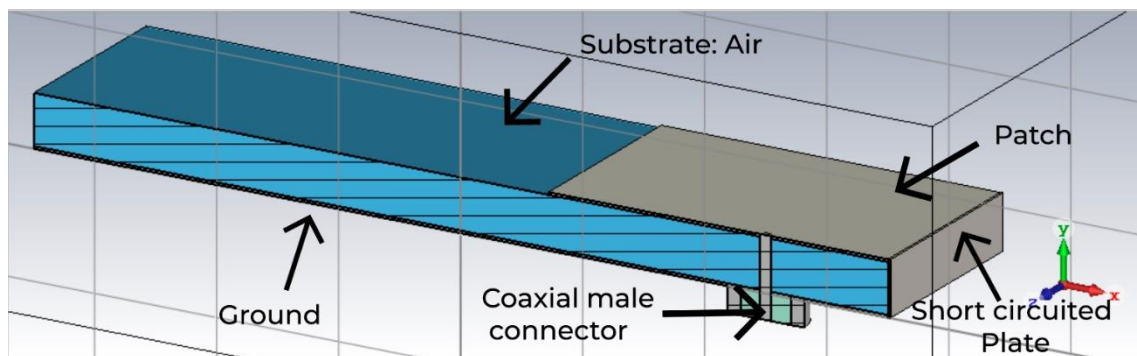


**Figure 13-Microstrip antenna modeling**

The dimensions of this antenna, in absolute values, are not small enough to be used in medical implants, however it helps us to have a better understanding of the simulation environments and the characteristics of planar antennas. If we want to make the antenna smaller we can change the material of the substrate. By changing the material, and therefore its electrical permittivity, you can make wavelength acquire lower values for a given frequency, making the antenna, in relative terms, smaller electrically and thus have a greater reduction margin to miniaturize it.

The structure of this antenna contains a plate that connects the patch to the ground by shorting them. According to the distribution of the electric field stored in a medium lambda half micro-strip, in the middle of the longitudinal section of the patch there is no E-field. This allows for the convenient installation of a conductive plate that connects the patch to the ground. Thus, we have kept only half of what would be a lambda/2 microstrip, having one now of lambda/4 that we have connected to ground, as if it was a monopole.

Here we can see the 3D radiation pattern of the y-axis oriented antenna in free space at a frequency of 2.45 GHz.



| farfield (f=2.45) [1] | |
| --- | --- |
| Type | Farfield |
| Approximation | enabled (kR >> 1) |
| Component | Abs |
| Output | Directivity |
| Frequency | 2.45 GHz |
| Rad. Effic. | -0.04516 dB |
| Tot. Effic. | -0.07719 dB |
| Dir. | 4.564 dBi |
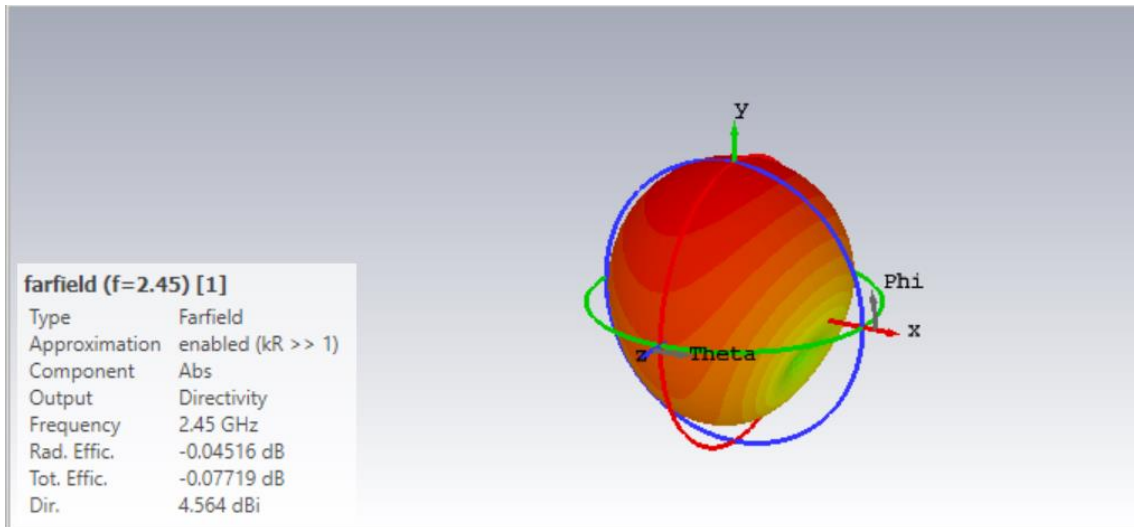
Figure 14- Radiation pattern of the microstrip antenna, 3D view.

We can also see it in 2D. In this case we can see the ZY plane which is the most interesting one. The antenna has only one main lobe in phi=90 and theta from 0 to 180 degrees. The main lobe, up until it falls 3 dB (half of the power) has an angular width of 162.5 degrees.
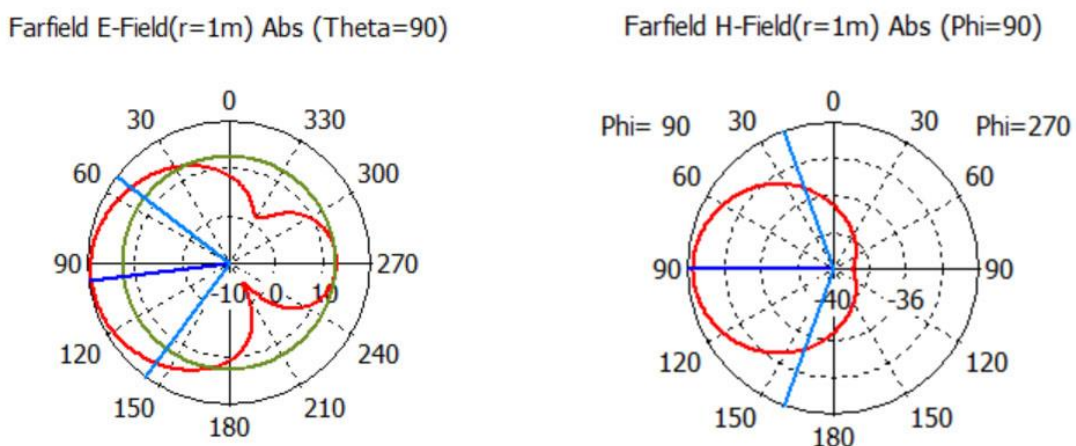


Figure 15- Radiation pattern of the microstrip antenna, polar view, E field and H field.

In order to calculate the longitudinal dimension of the patch and to adjust it to the desired frequency of 2.45 GHz where it must be resonant, it has been necessary to make several simulations by changing the length between ranges and by limiting the margins. We can see it in the following image:
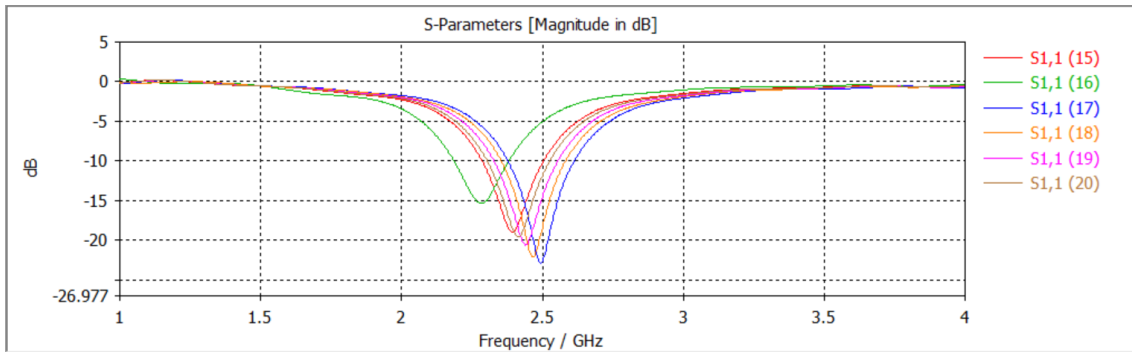


**Figure 16- Parameter s11 for different lengths.**

Once the length of the patch has been adjusted (length=27.88 mm), the position of the feeding point must be set. The position of the connector will determine the adaptation of the antenna to the line, in our case 50 ohms. As we have seen in Chapter 2, the ideal is that the impedance of the antenna is purely real and equal to the characteristic impedance of the line. In this way, the impedance seen from the generator will be equal to the impedance of the antenna regardless of the length of the cable. We have found a good solution by placing the connector 10 mm from the plate in the -x direction.

As we can see, at 2.45 GHz, we are approaching the real 50 ohms although we have some imaginary part. We have to take into account that simulations with prototypes are quite far from theoretical calculations in the same way that physical prototypes performances are far from simulations results. This may be because the thickness of the conductors induces capacitive loads.
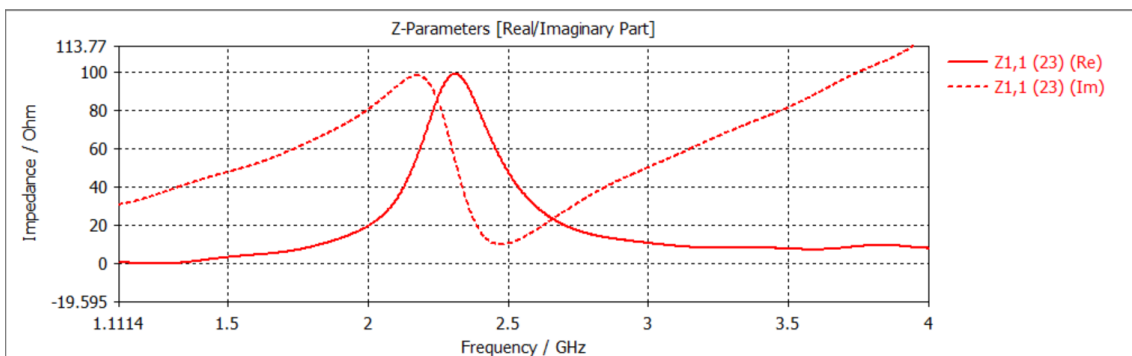


**Figure 17- Z11 parameter for length of the patch=27.8 mm**

In short, matching the impedances will also make that, by definition of the parameter $S_{11}$, it will approach values close to 0 in linear or high negative values in dBs, which means that almost all the energy transmitted to the antenna, will not be reflected.

Taking the criterion that the antenna works correctly with a parameter S11 below -10 dB, we have been able to obtain with Matlab the following data:
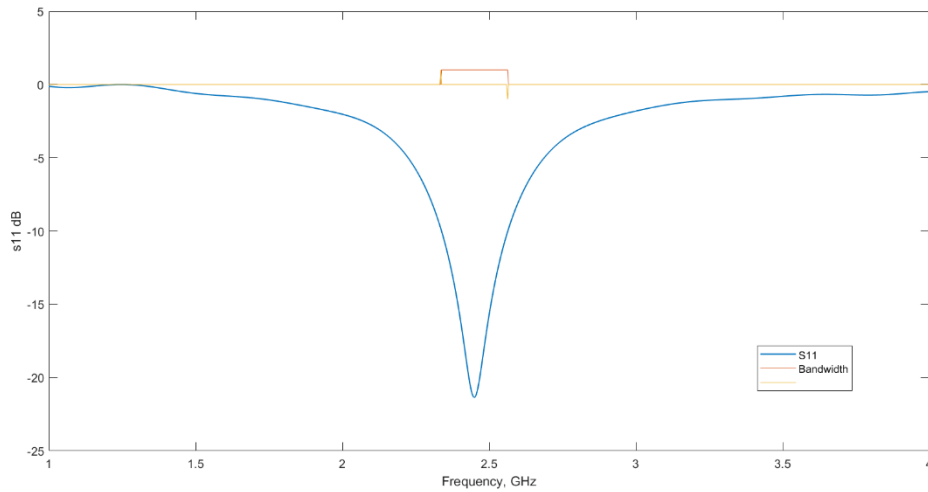


**Figure 18- s11 parameter and working frequencies, ploted in Matlab.**

| Cutoff Frequency 1 (GHz) | Cutoff Frequency 2 (GHz) | Bandwidth (GHz) |
|---|---|---|
| 2.3350 | 2.5630 | 0.2280 |

**Table 2- Bandwidth and cutoff frequencies of the microstrip antenna.**

**Human body modeling, encapsulation and cable**

The modeling of bodies and objects in the CST can be done through common and simple mathematical volumes such as spheres, cylinders, toroids, cones or cubes. In addition, each component can be a mix of them, doing addition or subtraction operations to combine them.

For our purpose (to see how human tissue affects the propagation of an electrically small antenna), no complex modeling of the human body in detail is necessary, simply a solid made of a material with losses similar to those of the human body. However, more complex models can be made in CST. For example, CST has a Voxel Family that contains 7 human models of different shapes and ages. These models contain 135 different tissues with which they form the organs, distributed in several million voxels. These models, composed of small cubes, are usually used to study exposure to ionizing radiation, radiation therapy and many other applications.
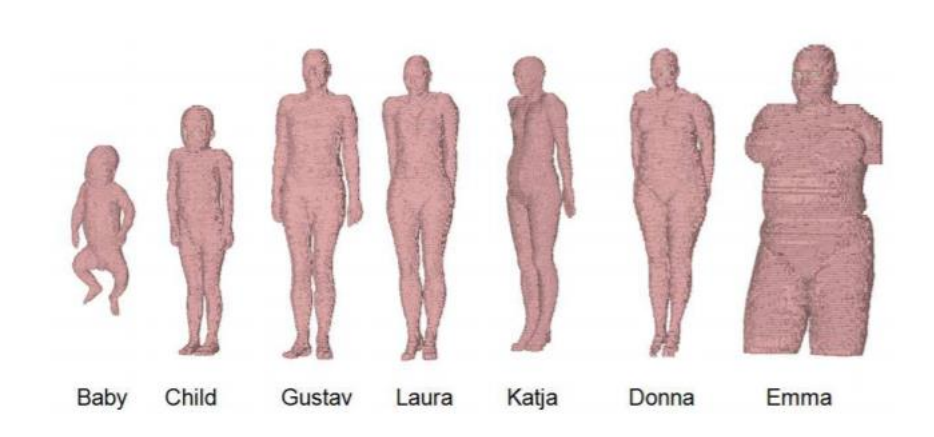
Figure 19- Voxel Family in CST. Source [17]

We, on the other hand, have simulated a simplification of the human body by means of a cylinder of 90 mm radius, composed of a customized material with the permittivity $|\varepsilon_r| = 41.3628$ and a Loss Tangent $tan\delta = 0.3367$, in other words, $\varepsilon_{r,body} = 39.20$-j13.20 at frequency 2.45 GHz (the values correspond to IEEE Head model [18]).
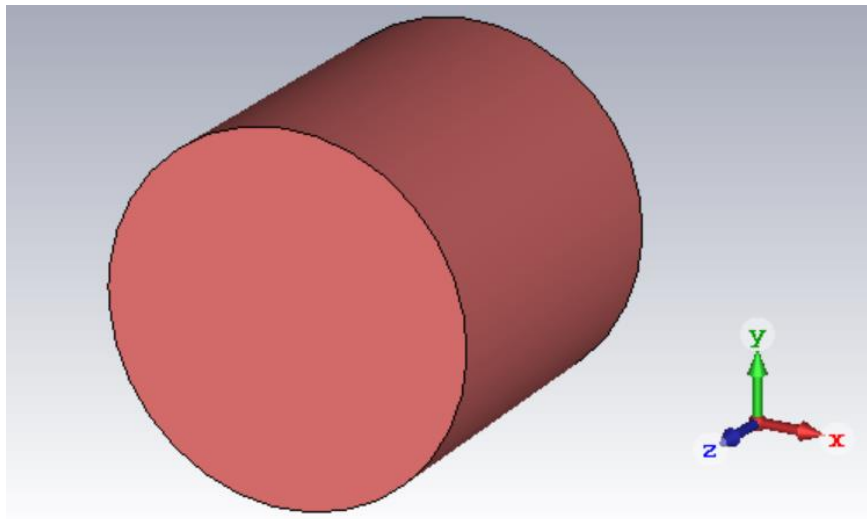


Figure 20- Body modeling.

Inside the body we'll find the antenna. The antenna is a lambda/4 dipole antenna. As we have already explained, we will prioritize the size of this antenna (that reaches 30 mm,) rather than having an s11 parameter centered on 2.45 GHz (in that case, antenna's length would be higher). The cylinder has its length oriented in the Z axis. This axis will also be the orientation of the antenna so that it radiates in all the body symmetrically when it is in the center.

The antenna, to simplify the simulations, has been constructed with a single ideal wire of lambda/4 (30.6122 mm) (full details in the construction of a dipole have not been taken into

account, but this study was seen in the previous section for the calculation of the parameter s11.

The antenna, so that it does not short-circuit with the human body, must be inside an encapsulation that prevents it from touching the body. This encapsulation has been the subject of study and we have varied its shape and volume. The encapsulation has been done through a subtraction of a cylindrical body to the body model. The material of the encapsulation is air, with a permittivity $\varepsilon_{r,air} = 1$.

The encapsulations we have made have been mostly z-axis oriented cylinders, like the rest of the body, and are subtractive solids from the body solid. So:

$$Component_{body} = Cylinder1_{body} - Cylinder2_{encapsulation}$$
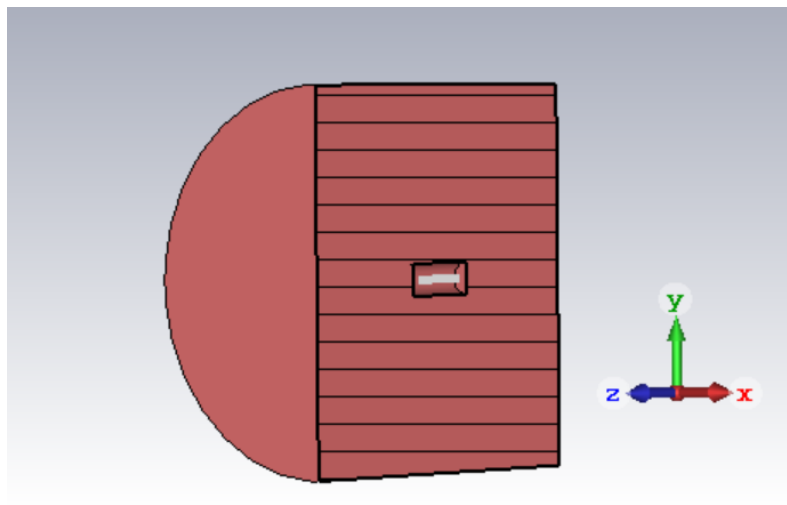


**Figure 21- Body modeling, encapsulation and wire dipole. Cut plane.**

In case the encapsulation is pillshaped, it is necessary to create the rounded shape of the edges by subtracting two spheres and a cylinder.

$$Component_{body} = Cylinder1_{body} - Cylinder2_{encap} - Sphere1_{enc} - Sphere2_{enc}$$
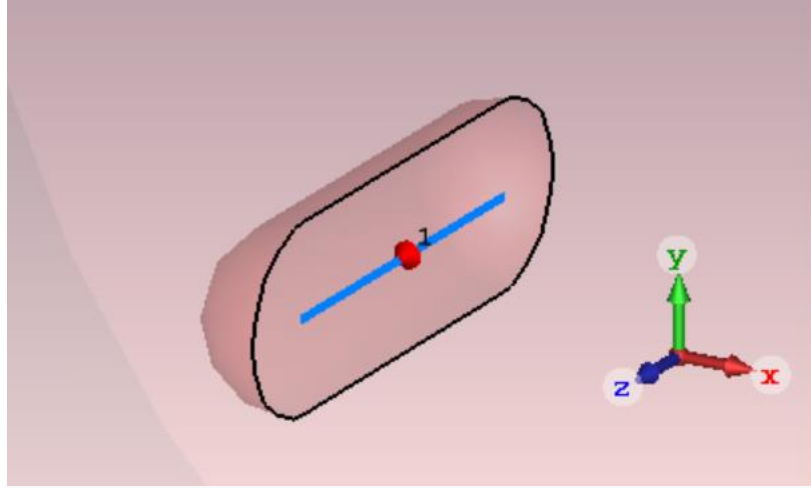
**Figure 22- Pill shape and wire dipole. Cut plane.**

In a general way and taking into account the encapsulation is going to move towards the edge of the body (the position changes) we can describe it as:

$$Component_{body} = Cylinder_{body}(r, z_{min}, z_{max}) - Encapsulation(r, y_{center}, z_{min}, z_{max})$$

Cylinder body is normally defined with constant parameters. In most simulations it has a length of $r = 90mm$ and length $= ||z_{max}| - |z_{min}|| = 2r = 180$mm.

The encapsulation varies in volume, so the radius or length varies. It also varies the position, which in this case is on the y-axis. The encapsulation and the antenna move progressively to the edges of the $Cylinder_{body}$ at a $step = 0.75\ mm$ so:

$$Encapsulation(r, n \cdot step, z_{min}, z_{max})$$

$$n = 0\ to\ N$$

Thus, the distance the wave has to travel from the origin and the thickness of human tissue (shorter distance) is:

$$distance\ covered = radius_{body} - n \cdot step$$

$$human\ tissue\ thickness_{shortest\ path} = radiusbody - n \cdot step - r_{encapsulation}$$
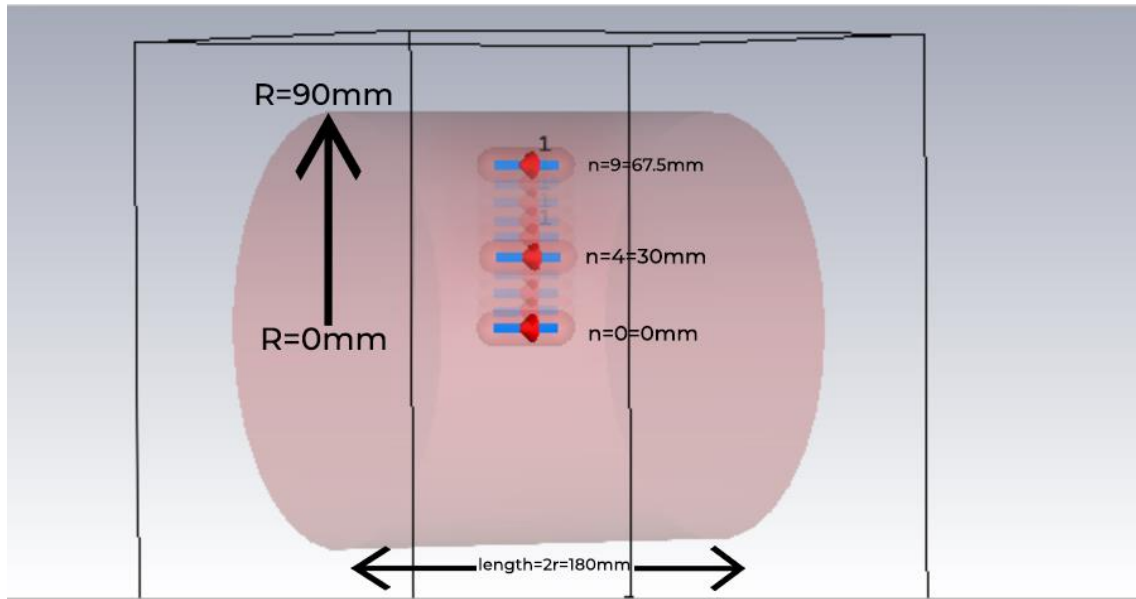
**Figure 23- Body modeling, different position of the encapsulation.**

## Results in CST

In this section we are going to observe the results of the efficiency that we have obtained with the modeling of the body already commented and a lambda/4 dipole for a frequency of 2.45 GHz. The simulations have been made as a function of the position and volumes of the different encapsulation. A total of 10 simulations have been performed for each encapsulation at a constant step, with a total of 5 different encapsulations.

The package and antenna have been moved at a constant 0.75 mm step in the y-axis direction, while the antenna is oriented in the z-axis. This means that it is the YZ plane that we are interested in at radiation pattern level. In spherical coordinates it means travelling through Theta from 0 to pi for a constant angle phi, which has values of 90 and 270 degrees.

For the first standard volume from which we have derived the rest, we have chosen a cylindrical shape with a radius of 15 mm and a length of 40 mm, making a total volume of 7.07 cm$^3$ .

The rest of the encapsulations are derived from this first one. The volumes have been scaled maintaining a criterion of proportionality *k*, defined as the ratio of length and radius.

| Volume 1 (mm³) | Radius (mm) | Total Length (mm) | Shape | Body Radius (mm) | k=l/r |
|---|---|---|---|---|---|
| 7,07E+03 | 7,5 | 40 | Cylinder | 90 | 5,333333333 |
| | | | | | |
| Rad Efficiency (dB) | Total Efficiency (dB) | y-axis (mm) | Distance Antenna-Body Edge (mm) | Distance Encapsulation Edge- Body Edge (mm) | Directivity (dBi) |
| -64,85 | -98,31 | 0 | 90 | 82,5 | 3,733 |
| -51,7 | -85,17 | 7,5 | 82,5 | 75 | 8,893 |
| -45,15 | -78,37 | 15 | 75 | 67,5 | 10,45 |

31

| | | | | | |
|---|---|---|---|---|---|
| **-38,92** | -72,41 | 22,5 | 67,5 | 60 | 5,111 |
| **-36,48** | -69,95 | 30 | 60 | 52,5 | 8,277 |
| **-37** | -70,46 | 37,5 | 52,5 | 45 | 5,723 |
| **-33** | -66,46 | 45 | 45 | 37,5 | 4.292 |
| **-29,81** | -63,27 | 52,5 | 37,5 | 30 | 4,659 |
| **-27** | -60,53 | 60 | 30 | 22,5 | 4,532 |
| **-24,26** | -57,54 | 67,5 | 22,5 | 15 | 4,747 |

**Table 3- Results for Volume 1**

Two times volume 1: Volume 2, cylinder shape

| Volume 2 (mm³) | Radius (mm) | Total Length (mm) | Shape | Body Radius (mm) | k=l/r |
|---|---|---|---|---|---|
| **1,41E+04** | 9,4494 | 50,3968 | Cylinder | 90 | 5,333333333 |
| | | | | | |
| **Rad Efficiency (dB)** | Total Efficiency (dB) | y-axis (mm) | Distance Antenna-Body Edge (mm) | Distace Encapsulation Edge- Body Edge (mm) | Directivity (dBi) |
| **-69,82** | -104,4 | 0 | 90 | 80,5506 | 4,17 |
| **-60,3** | -94,76 | 7,5 | 82,5 | 73,0506 | 7,5 |
| **-46,37** | -80,35 | 15 | 75 | 65,5506 | 9,728 |
| **-39,25** | -73,77 | 22,5 | 67,5 | 58,0506 | 6,735 |
| **-34,9** | -69,44 | 30 | 60 | 50,5506 | 7,103 |
| **-35,62** | -70,16 | 37,5 | 52,5 | 43,0506 | 5,899 |
| **-31,83** | -66,35 | 45 | 45 | 35,5506 | 4 |
| **-28,53** | -63,05 | 52,5 | 37,5 | 28,0506 | 4,656 |
| **-25,62** | -60,17 | 60 | 30 | 20,5506 | 4,467 |
| **-23,16** | -57,3 | 67,5 | 22,5 | 13,0506 | 4,714 |

**Table 4- Results for Volume 2**

Three times volume 1: Volume 3, cylinder shape

| Volume 3 (mm³) | Radius (mm) | Total Length (mm) | Shape | Body Radius (mm) | k=l/r |
|---|---|---|---|---|---|
| **2,12E+04** | 10,81687178 | 57,69 | Cylinder | 90 | 5,333334922 |
| | | | | | |
| **Rad Efficiency (dB)** | Total Efficiency (dB) | y-axis (mm) | Distance Antenna-Body Edge (mm) | Distace Encapsulation Edge- Body Edge (mm) | Directivity (dBi) |
| **-74,53** | -108,6 | 0 | 90 | 79,18312822 | 4,821 |
| **-64** | -99,97 | 7,5 | 82,5 | 71,68312822 | 7,034 |
| **-44,65** | -78,68 | 15 | 75 | 64,18312822 | 10,37 |
| **-40,65** | -74,68 | 22,5 | 67,5 | 56,68312822 | 8,981 |
| **-35,2** | -69,24 | 30 | 60 | 49,18312822 | 5,986 |
| **-35,74** | -69,77 | 37,5 | 52,5 | 41,68312822 | 5,898 |
| **-32,26** | -66,29 | 45 | 45 | 34,18312822 | 4 |
| **-28,87** | -62,88 | 52,5 | 37,5 | 26,68312822 | 4,586 |

| -25,93 | -59,93 | 60 | 30 | 19,18312822 | 4,492 |
| -22,73 | -56,83 | 67,5 | 22,5 | 11,68312822 | 4,764 |

**Table 5- Results for Volume 3**

Half times volume 1: Volume 1/2, cylinder shape

| Volume 1/2 (mm³) | Radius (mm) | Total Length (mm) | Shape | Body Radius (mm) | k=l/r |
|---|---|---|---|---|---|
| 3,53E+03 | 5,9528 | 31,748 | Cylinder | 90 | 5,333288536 |
| | | | | | |
| Rad Efficiency (dB) | Total Efficiency (dB) | y-axis (mm) | Distance Antenna- Body Edge (mm) | Distace Encapsulation Edge- Body Edge (mm) | Directivity (dBi) |
| -48,84 | -79,18 | 0 | 90 | 84,0472 | 4,075 |
| -45,04 | -75,38 | 7,5 | 82,5 | 76,5472 | 9,826 |
| -40,52 | -70,88 | 15 | 75 | 69,0472 | 5,576 |
| -39,41 | -69,75 | 22,5 | 67,5 | 61,5472 | 8,621 |
| -41,07 | -71,41 | 30 | 60 | 54,0472 | 4,53 |
| -38,03 | -68,36 | 37,5 | 52,5 | 46,5472 | 4,719 |
| -34,68 | -65,01 | 45 | 45 | 39,0472 | 4,437 |
| -32,05 | -62,41 | 52,5 | 37,5 | 31,5472 | 4 |
| -29,01 | -59,36 | 60 | 30 | 24,0472 | 4,931 |
| -25,77 | -56,08 | 67,5 | 22,5 | 16,5472 | 4,328 |

**Table 6- Results for Volume 1/2**

One time volume 1: Volume 1, pill shape

| Volume 1 (mm³) | Radius (mm) | Total Length (mm) | Shape | Body Radius (mm) | k=l/r |
|---|---|---|---|---|---|
| 7,07E+03 | 7,8414 | 41,8206 | Pill | 90 | 5,333307828 |
| | | | | | |
| Rad Efficiency (dB) | Total Efficiency (dB) | y-axis (mm) | Distance Antenna- Body Edge (mm) | Distace Encapsulation Edge- Body Edge (mm) | Directivity (dBi) |
| -71,45 | -104,8 | 0 | 90 | 82,1586 | 2,732 |
| -57,67 | -91,07 | 7,5 | 82,5 | 74,6586 | 8,126 |
| -44,61 | -77,96 | 15 | 75 | 67,1586 | 10,76 |
| -40,94 | -74,28 | 22,5 | 67,5 | 59,6586 | 7,905 |
| -36,23 | -69,58 | 30 | 60 | 52,1586 | 6,478 |
| -37,52 | -70,86 | 37,5 | 52,5 | 44,6586 | 6,149 |
| -33,68 | -67,03 | 45 | 45 | 37,1586 | 4,134 |
| -30,27 | -63,6 | 52,5 | 37,5 | 29,6586 | 4,637 |
| -27,41 | -60,8 | 60 | 30 | 22,1586 | 4,536 |
| -24,46 | -57,88 | 67,5 | 22,5 | 14,6586 | 4,747 |

**Table 7- Results for Volume 1 , pill shape**

## Radiation Pattern

In the radiation pattern we can see how the power is distributed around the antenna. As we have said before, as the antenna is oriented in z and moves in y direction, the ZY plane is relevant.

The diagram shows how many lobes there can be around the antenna. In other words, it shows us which areas have more directed power. If all power is distributed equally in all directions, we are talking about an isotropic antenna.

To represent the radiation diagrams we have collected a 3D image, a 2D image in polar format and a Matlab process that recognizes the relevant lobes of the diagram. In the latter case it is set with Cartesian axes, where the x-axis represents the angles in pi/rad and the y-axis represents the dBi (with respect to an isotropic antenna).

The following magnets show the radiation pattern of the cylinder with volume 1 located in the center of the body :
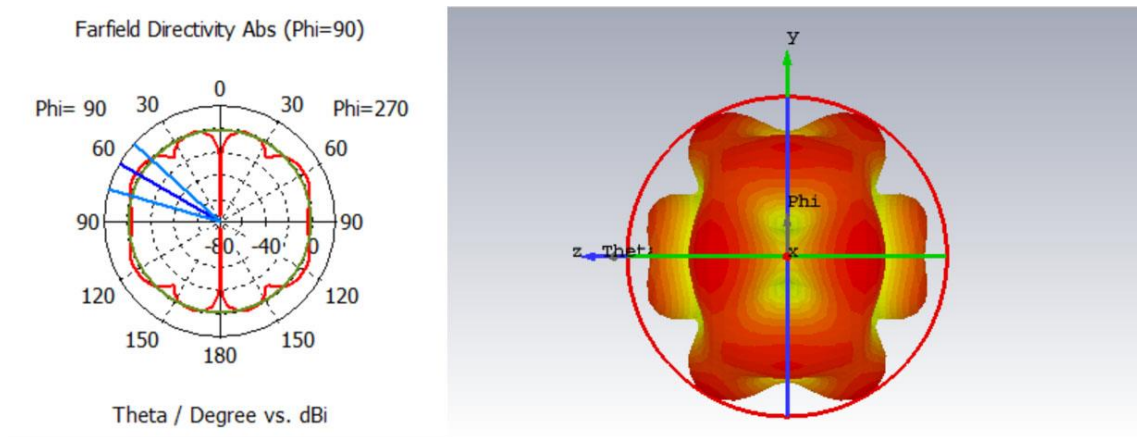


**Figure 24-Polar and 3D representation of radiation pattern, E-Plane. Position: center.**
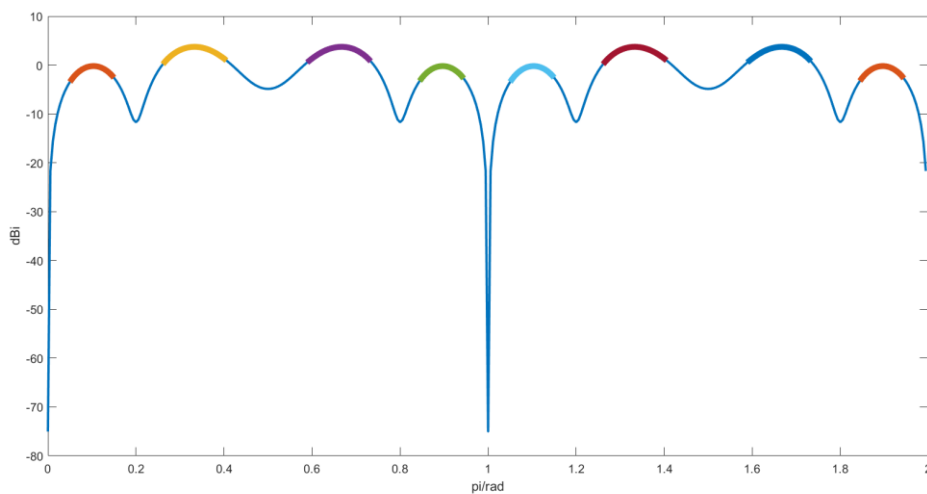


**Figure 25- Cartesian representation of radiation pattern (E-Plane). Relevant lobes detected by Matlab function. Position: center.**

In the following images we see, the antenna radiating at 3 centimeters from the center, we observe how the symmetry disappears and the antenna becomes more directive:
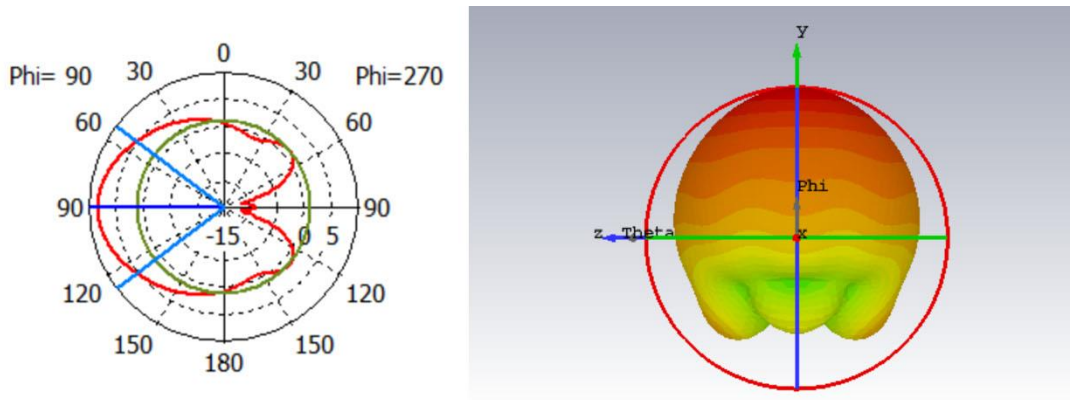


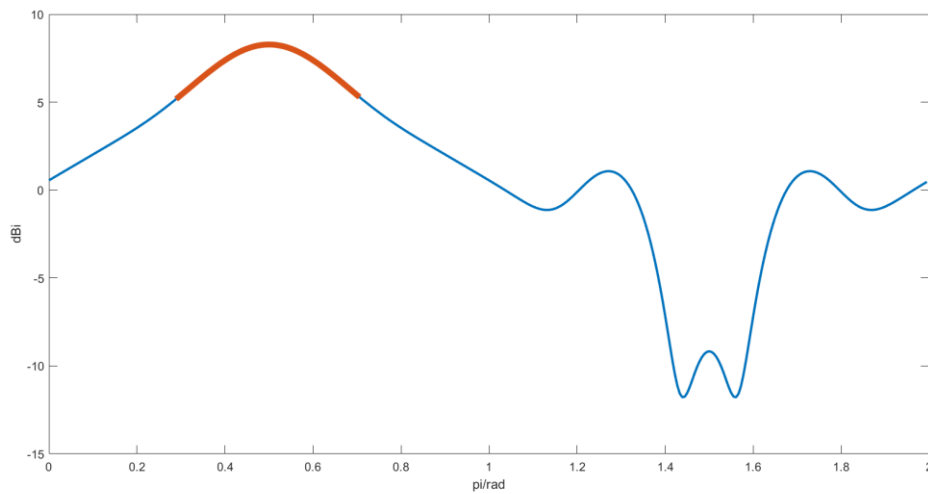**Figure 26-Polar and 3D representation of radiation pattern, E-Plane. Position: 3 cm.**



**Figure 27- Cartesian representation of radiation pattern (E-Plane). Relevant lobes detected by Matlab function. Position: 3 cm.**

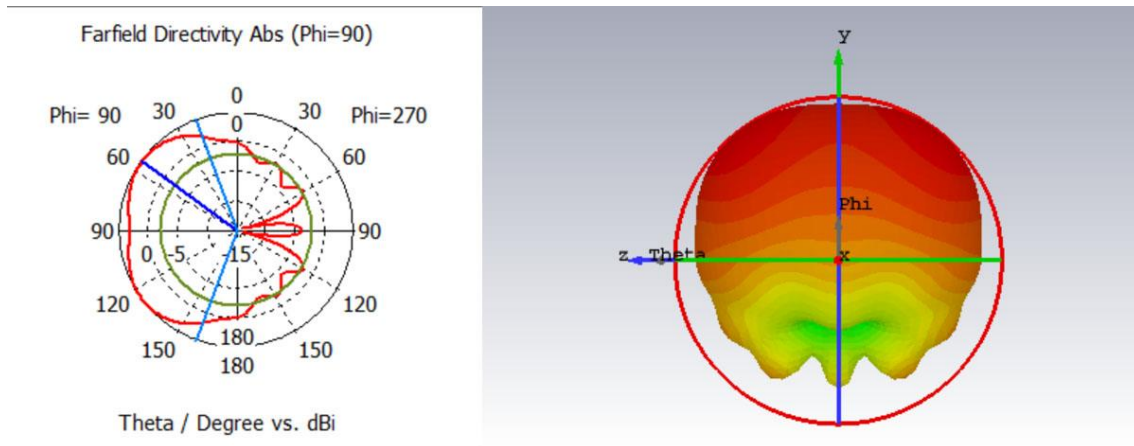Finally we see how it behaves 6.75 cm from the center of the cylinder that simulates our human body:

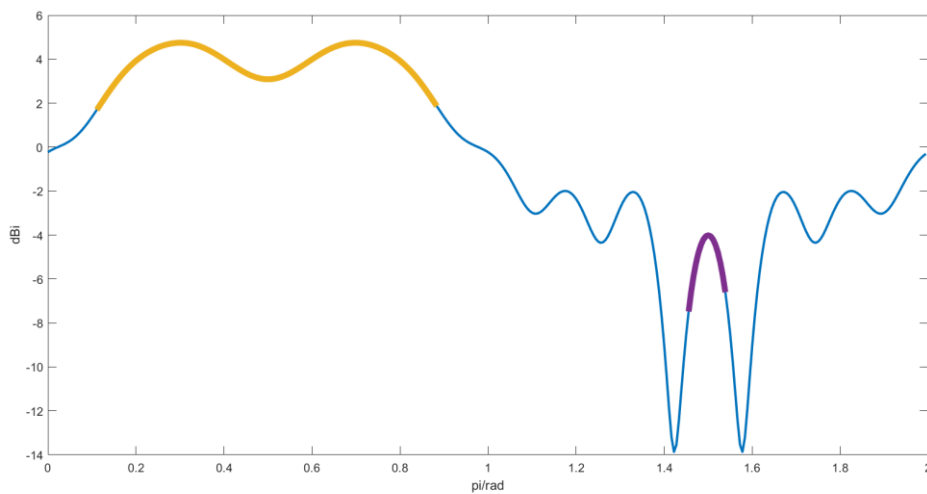**Figure 28-Polar and 3D representation of radiation pattern, E-Plane. Position: 6.75 cm.**



**Figure 29- Cartesian representation of radiation pattern (E-Plane). Relevant lobes detected by Matlab function. Position: 6.75 cm.**

In this last image we see all the radiation diagrams overlapped in a Cartesian plane, processed with Matlab. Although it is true that, in a general way, the antennas are more directive in any position far from the center where they lose the radiation symmetry, there are many ways in which the radiation pattern behaves and it would be necessary to establish a compromise between the directivity we are interested in for our system and the efficiency it offers.
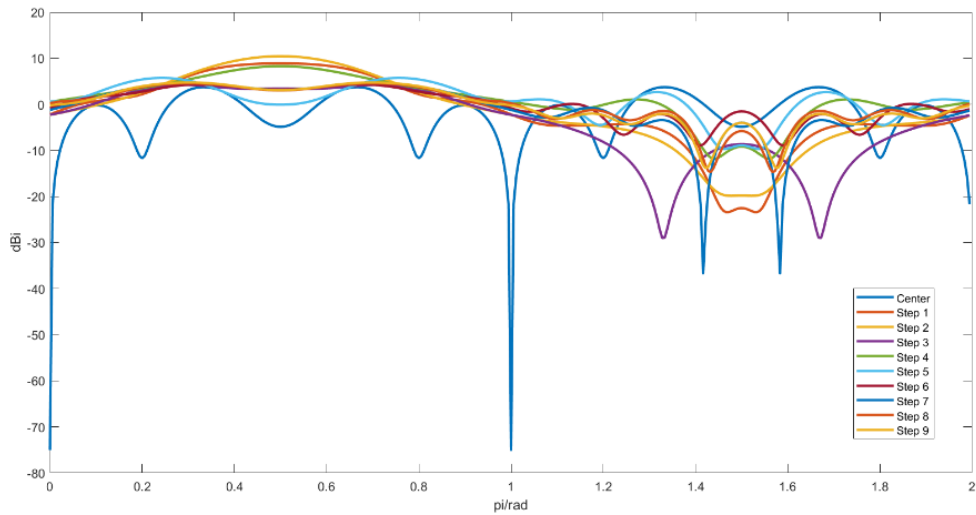
**Figure 30- Radiation patterns of the E-Plane overlaped. 2D representation.**

## Efficiency

In this graph we see the different efficiencies for the different volumes described above. On the x-axis is represented the position of the antenna in millimeters with respect to the center of the body (position 0). The y-axis represents the radiated efficiency in dBs.

As we can see, the individual trend of each graph is clear: the efficiency improves, as we expected, as we move away from the center and approach the outside, since the signal must pass through less thickness of human body.

However, something that was not expected to be observed is that small volumes are more efficient than larger ones in the center of the body and up to 1-2 centimeters away from the center. This may be due to the symmetricity of the propagation in the center in the radiation pattern, which disappears as we move away.
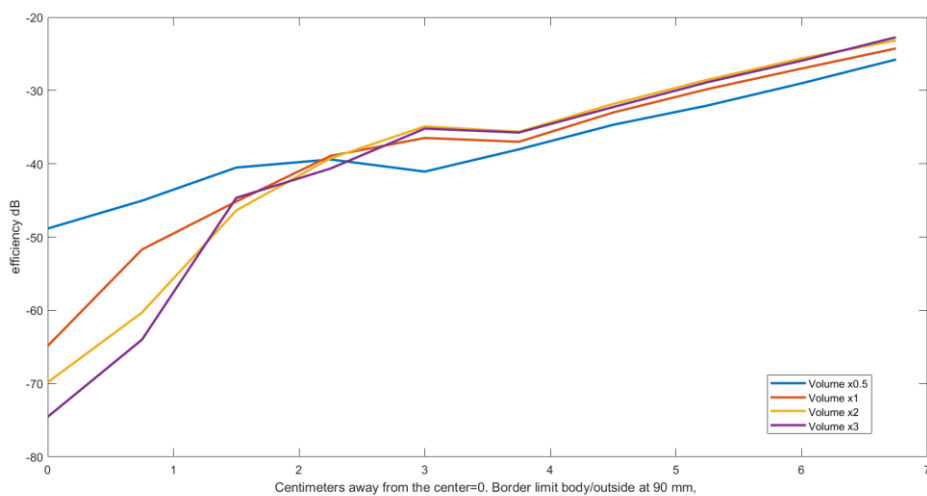


**Figure 31- Efficiency in different positions (x-axis), and different volumes (each line).**

In this following graph we see the comparison between volume 1 in cylinder form and the same volume in tablet form (in the following chapter you can see the criteria for shape transformation).

Differences in efficiency depending on the shape are practically non-existent from 3 centimeters away from the center. However, the same cannot be said for the centre of the body where symmetries occur. The pill shape is much less efficient than the cylindrical shape.
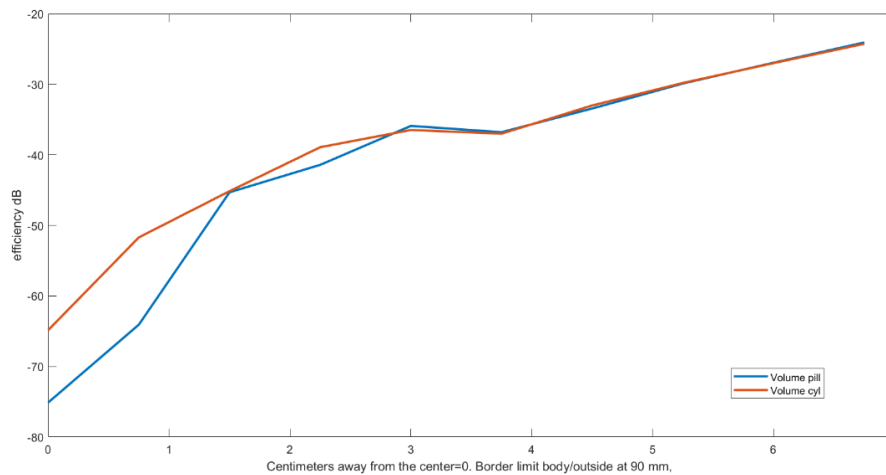


**Figure 32- Efficiency in different positions (x-axis) for a certain volume but different shapes (Cylinder and Pill shape).**


**Directivity**

The Directivity of an antenna is defined as the ratio of the power density radiated in one direction, at one distance, to the power density that an isotropic antenna would radiate at the same distance, at equal total radiated power. Usually we refer to directivity in the direction whose power value is maximum. The logical thing would be to orient our antenna, if possible, both receiving and transmitting in this direction so that the link is the best possible. Directivity therefore, when compared to the isotropic antenna, which radiates equally in all directions, will be measured in dBi and not in dB.

In the following graph we can see the value of the directivity for each cylindrical volume. The y-axis represents the power in dBi and the x-axis represents, as we have been doing, the distance from the center of the body.
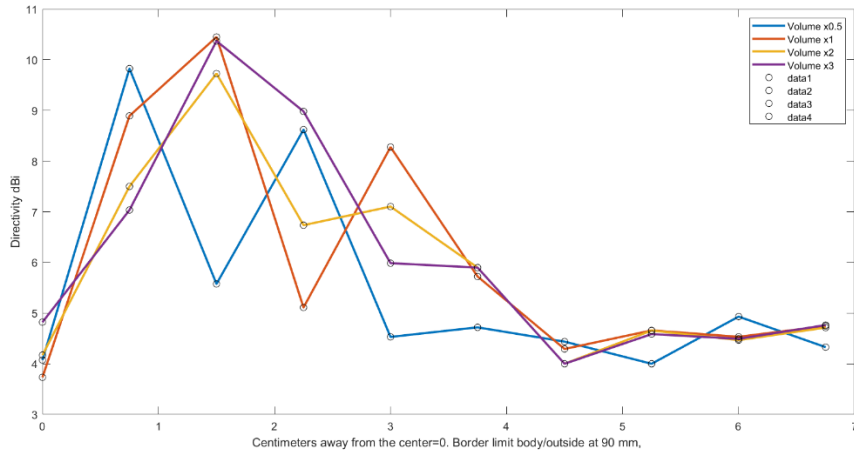
**Figure 33- Directivity in different positions (x-axis), and different volumes (each couloured line).**

As we had already observed in the radiation diagram, despite the loss of symmetry as you move away from the centre and the radiation in the direction -y is of a very poor quality, the directivity does not seem to increase clearly as you move away from the centre. If it were to increase progressively, we would end up with a very narrow main-lobe antenna with a very high directivity.

In the graph we see how the directivity increases by 1.5 cm in all the encapsulations but then decreases to values around 4-5dBi from 4.5 cm.

# Chapter 4: Use and techniques in Matlab for the interpretation of results

**Parameter s11**

As we have seen in previous sections, the CST program offers us a graph where the parameter s11 appears, which is the absolute value of the reflection coefficient. In order to deal better with the data and to be able to establish criteria of a good operation, a Matlab script has been made to manage this data. CST offers an export to a .txt ASCII file in which two columns of data appear: the value in dBs of the parameter s11 and the frequency to which this value corresponds.
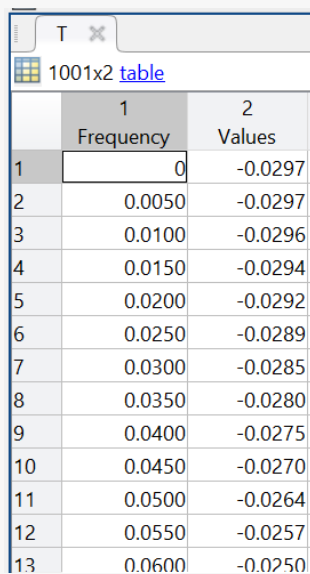
By using the importdata command and classifying it into a table by using table, Matlab is able to read the .txt file and classify it into a table with two columns: frequencies and the value in dBs.

So, being able to classify our data, we can make a script with which we can put two input parameters: the name of the file and the maximum level of dBs that we are willing to tolerate and it will take out the cut-off frequencies and the bandwidth in the working frequencies.
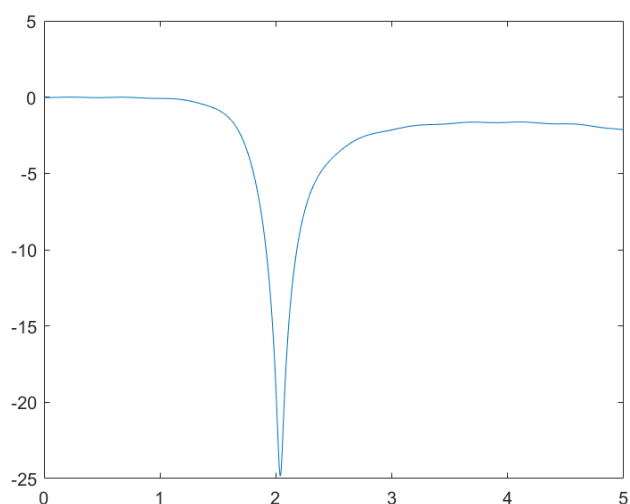
```
function [bandwidths, cutoff_frequency_1, cutoff_frequency_2] =
Bandwidth_dB(filename, dB_limit)
```

With the classified data we then obtain 2 column vectors of 1001 values that we can represent:

```
T = CST2Table(filename);
plot(T.Frequency, T.Values)
hold on
```



In this vector of values, we can check which values are below the dB limit we have chosen. We can do this by constructing a Boolean vector of 0s and 1s. The vector will be worth 1 if

it satisfies the condition (being below the dB_limit, so it is within the working frequency range) and 0 if it does not.

*Given a vector X with N elements $\epsilon \ \mathbb{R}$, boolean vector B will be a vector with N elements*

$$where \ \begin{cases} b_n = 1, & if \ \ x_n < -dB_{limit} \\ b_n = 0, & if \ \ x_n \geq -dB_{limit} \end{cases}$$

```
boolean_dB = T.Values < -dB_limit;
plot(T.Frequency, boolean_dB)
```
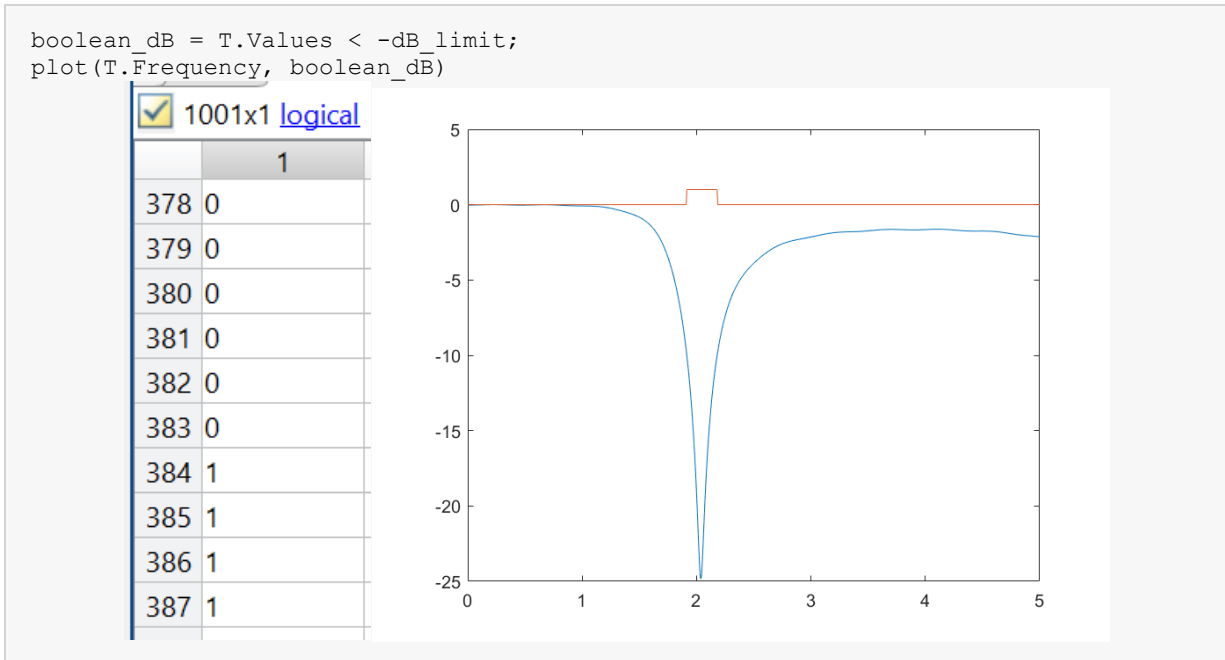


In case there is only one valley, we can easily determine the bandwidth and cut-off frequencies by using the find function and the 'first' and 'last' tags. Where we will look for the first and last 1 of the previous Boolean vector, to determine the position of where the range of working frequencies starts and ends.

```
first_dB=find(boolean_dB==1, 1, 'first');
last_dB=find(boolean_dB==1, 1, 'last');
bandwidth=T.Frequency(last_dB)-T.Frequency(first_dB);
cutoff_frequency_1=T.Frequency(first_dB);
cutoff_frequency_2=T.Frequency(last_dB);
```

However, what happens if the antenna has more than one bandwidth in which it can work properly? In that case, we must solve the problem in another way and detect how many valleys we have, where they start and where they end. We can see the following procedure:

*Given a boolean vector $B = [b_1, b_2, b_3 \dots b_n, \dots b_N]$ of N elements*

*We can derive 2 more vectors $B_{mod,1}$ and $B_{mod,2}$ with $N - 1$ elements*

$$B_{mod,1} = [b_2, b_3, b_4, \dots, b_n, \dots b_N]$$

$$B_{mod,2} = [b_1, b_2, b_3, \dots, b_n, \dots b_{N-1}]$$

*If we substract $B_{mod,1} - B_{mod,2}$, then, the result is another vector C of $N - 1$ elements*

*C is not a boolean vector and it has only 3 different values*:

$$\left\{ \begin{array}{l} C_n = 1, indicates\ the\ beggining\ of\ a\ valley \\ C_n = -1, the\ end\ of\ a\ valley \\ C_n = 0, no\ changes\ on\ tendency \end{array} \right.$$

*Finallly, we can express*

$$Cutoff\ Frequency\ Starts_{indexes} = n \rightarrow indexes\ values\ of\ C(n)\ where\ c_n = 1$$

$$Cutoff\ Frequency\ Ends_{indexes} = n \rightarrow indexes\ values\ of\ C(n)\ where\ c_n = -1$$

$$Bandwidths = Cutoff\ Frequency\ Starts - Cut\ off\ Frequency\ Ends$$

```
change = boolean_dB(2:end) - boolean_dB(1:end-1);


plot(T.Frequency(1:end-1), change)


hold on
xlabel('Frequency, GHz')
ylabel('s11 dB')
legend({'S11','Boolean vector B', 'Change vector C'})
starts = find(change == 1);
ends = find(change == -1);

num_valleys = length(starts);

bandwidths = zeros(num_valleys, 1);
cutoff_frequency_1=zeros(num_valleys, 1);
cutoff_frequency_2=zeros(num_valleys, 1);
for i = 1:num_valleys
    bandwidths(i) = T.Frequency(ends(i)) - T.Frequency(starts(i))
    cutoff_frequency_1(i)=T.Frequency(starts(i))
    cutoff_frequency_2(i)=T.Frequency(ends(i))
end
```
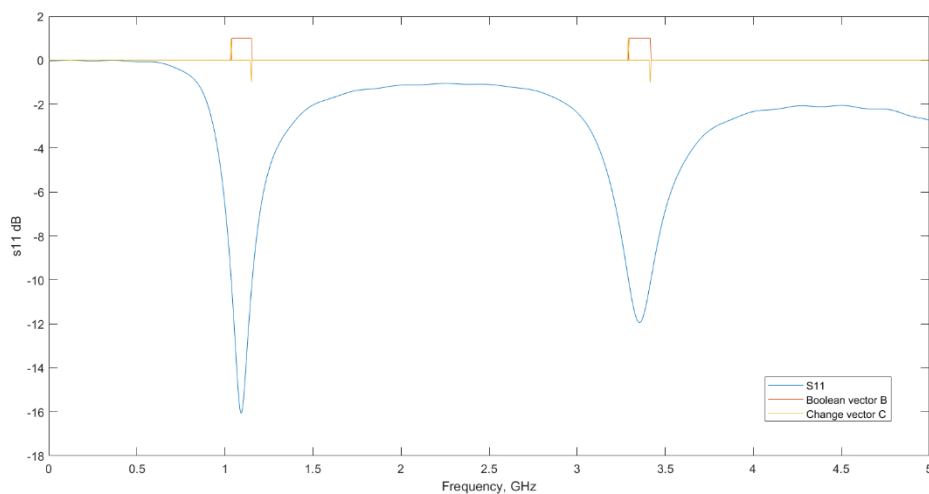
**Radiation diagram on Matlab**

In the same way that we have been able to export the data of parameter s11 of the CST to an ASCII .txt document, we have done the same for the radiation pattern and plot the number of lobes that are present according to an arbitrary limit (dBLimit) that indicates what we consider part of the lobe.

In other words, if we have a maximum of one lobe at a given theta angle, that lobe will exist in a range of degrees whose limits are determined by the Maximum Value [dBi]-dBLimit [dB]. Typically a range of -3 dB (half the power) is taken as the useful range of one lobe. That is, at the moment the power drops by half, we can say that the lobe ends.

The first step is also to move from text format to table format. We use this function created CST2Table that makes use again of the importdata and table commands with the input: file.txt and we classify it in a table where only the theta values and the absolute value of the dBi level will be useful for the radiation pattern.

$Vector\ Theta = [0, 1, 2, 3, \ldots, 178, 179, 180, 179, 178, \ldots 4, 3, 2, 1]$ with N= 360 elements

$$Theta_{\varphi=90°} = Theta(n_1\ to\ n_{180})$$

$$Theta_{\varphi=270°} = Theta(n_{181}\ to\ n_{360})$$

```
176.000        90.000        -1.026e+00
177.000        90.000        -1.170e+00
178.000        90.000        -1.316e+00
179.000        90.000        -1.464e+00
180.000        90.000        -1.616e+00
179.000       270.000        -1.771e+00
178.000       270.000        -1.929e+00
177.000       270.000        -2.090e+00
```

**Figure 34- Part of Txt file of Radiation pattern**

To reorder the Theta vector from 0 to 360 degrees we make the following transformation:

$$Theta_{360°} = [Theta_{\varphi=90°}, (Theta_{\varphi=270°}(n_{360}, n_{181}) + 180°)]$$

We can also express it in terms of $\pi/rad$:

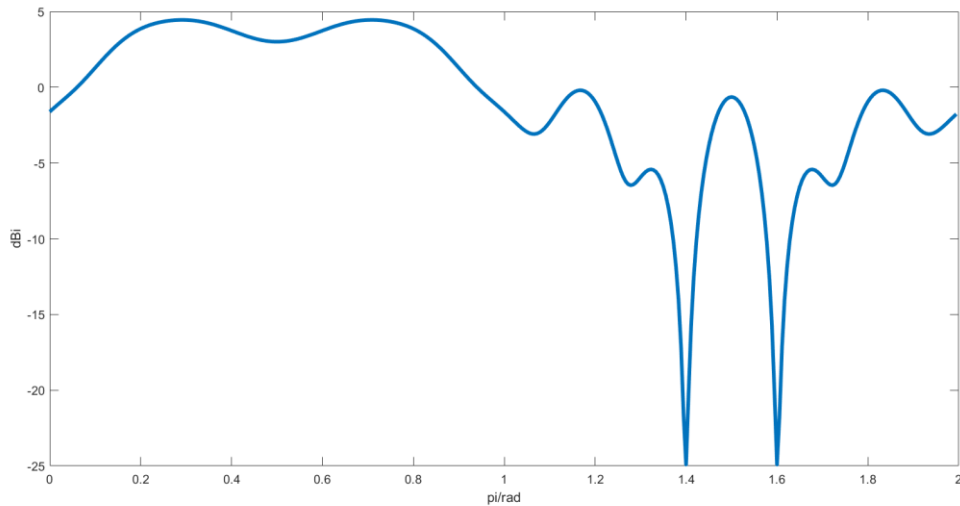$$Theta_{\pi/rad} = \frac{Theta_{360°}\ \pi}{180}$$

```
T=CST2Table_radiation_pattern(filename);
theta_rad_180=T.Theta*pi/180;
theta_rad_aux=fliplr((theta_rad_180(182:end)+pi)');
theta_rad_360=[theta_rad_180(1:181)',theta_rad_aux]/pi;
```

```
plot(theta_rad_360, T.Abs)

xlabel('pi/rad')
ylabel('dBi')
hold on
```



In case the radiation pattern has only one relevant lobe, establishing which is the main lobe is a relatively easy task, because it would be enough to find the maximum power value in dBi and establish a range of -3 dB (for example) from the maximum value. There would only be one main lobe, as it would be the only one that would meet the requirements.

$$Given\ those\ vectors:$$

$$V(values)[dBi]\ and\ Theta(0to2)[\pi/rad], both\ with\ N = 360\ elemets\ \ and\ a\ dB_{Limit}$$

Then: $m = maximum\ value\ of\ V$

$$Boolean\ vector\ B\ of\ N\ elemets\ where \begin{cases} b_n = 1, & if\ v_n > dB_{limit} \\ b_n = 0, & if\ v_n \le dB_{limit} \end{cases}$$

$$Cutoff\ angle_{1,index} = first\ n\ index\ value\ of B(n)\ where\ b_n = 1$$

$$Cutoff\ angle_{2,index} = last\ n\ index\ value\ of\ B(n)\ where\ b_n = 1$$

$$Cutoffangle_1 = Theta(theta_{Cutoffangle_{1,index}})$$

$$Cutoffangle_2 = Theta(theta_{Cutoffangle_{2,index}})$$

$$Bandwidth = Cuttoffangle_2 - Cutoffangle_1$$

```
max_dBi=max(abs_half);

boolean_dBi = abs_half>max_dBi-dB_limit;

cutoff_angle_aux1=find(boolean_dBi==1, 1, 'first');
cutoff_angle_aux2=find(boolean_dBi==1, 1, 'last');
cutoff_angle_1=theta_rad_360(cutoff_angle_aux1);
```

```
cutoff_angle_2=theta_rad_360(cutoff_angle_aux2);
beam_width=cutoff_angle_2-cutoff_angle_1;
```

However, it is most common for us to find more than one relevant main lobe that meets our dBLimit criteria. In this case it is necessary to then find, not only the maximum value of the vector of values but all the local maxima of the vector. For this we must make the first and second derivative of a vector with discrete values:

*Given a values $V(n)$ vector of 360 elements:*

*Cause is cylcical we extend the first value to the end of the vector*

$$V_{mod} = [v_2, v_3, v_4, \dots, v_{360}]$$

First Derivative auxiliar Vector $= V_{mod} - V$

We create a boolean vector B where $\begin{cases} b_n = 1, & if\ Fdav_n\ is\ positive\ (increasing) \\ b_n = 0, & if\ Fdav_n\ is\ negative\ (rest\ of\ cases) \end{cases}$

*For the second derivative we proceed similarly:* $B_{mod} = [b_2, b_3, b_4, \dots b_{360}, b_1]$

*Second Derivative Vector* $V'' = B_{mod} - B$

$$V''(n) = \begin{cases} 1, & if\ is\ a\ local\ minimum \\ -1, & if\ is\ a\ local\ maximum \\ 0, & if\ trend\ doesn't\ change \end{cases}$$

*Local Maximums$_{index}$* $= (n + 1)$ *and reffers to index values where* $V''(n) = 1$

```
function [local_maximums, local_minimums]=
findLocalZeroDerivativeCyclical(magnitude)
magnitude_new=[magnitude; magnitude(1)];

first_derivative=magnitude_new(2:end)-magnitude_new(1:end-1);
first_derivative_new=[first_derivative; first_derivative(1)];

boolean_increasing=first_derivative_new>0;
boolean_increasing_new=[boolean_increasing; boolean_increasing(1)];
boolean_trend_change=boolean_increasing(2:end)-boolean_increasing(1:end-1);

local_maximums=find(boolean_trend_change== -1)+1;
local_minimums=find(boolean_trend_change== 1)+1;
```

At this point we have a vector of indexes of local maximums. The next question at this point is: Are all the local maximums of radiation pattern a maximum of a lobe?

It depends depends on the criteria and what we consider a lobe, and it is defined with the dB Limit we introduce as an arbitrary variable. Tipically we can use -3dB as a limit.

In other words, we may have small disturbances or noise in our radiation pattern values. So we can say that, in undesirable measurements, not all local maximums of radiation pattern are the maximum of a real lobe, maybe they are little variations due to bad mesasurements. So to know if a local maximum is a maximum of a lobe or it is just a small and not relevant disturbance in our criteria, we proceed as follows:

Let's put an example:

$$Given\ a\ vector\ A = [0,0,2,3,4,5,6,5,7,4,2\ ,0,0,0]\ with\ N = 12\ elements$$

$$The\ local\ maximums\ of\ vector\ A\ are\ in\ positions\ n = \ 7\ and\ n = 9\ with\ values\ [6,7]$$

$$Local\ Maximum_{index} = [7,9]\ \text{(our candidates to be a maximum)}$$

$$If\ our\ dB\ Limit\ is\ 3dB, which\ values\ are\ greater\ than: A\big(Maximum_{vector}(n)\big) - 3dB?$$
$$When\ n = 1, We\ find\ values\ greater\ than\ A(7) - 3dB = 6 - 3dB = 3$$

$$Boolean\ vector\ B = [0,0,0,0,1,1,1,1,1,1,0,0,0]$$

$$In\ this\ section\ of\ ones, is\ B(7)\ (lobe\ around\ A(7) = 6)\ the\ maximum\ of\ the\ section\ of\ ones?$$
$$In\ this\ case\ is\ not\ the\ maximum, cause\ the\ maximum\ of\ the\ lobe\ is\ A(9) = 7$$

So if our candidate is the máximum of the section of (relevant values inside the lobe) we return a 1, if it is not, we discard it, 0 is returned and we check the next Local Maximum candidate because ther should be another local maximum that is the máximum of the lobe.

The general procedure is:

$$Given\ a\ dB\ Limit, and\ vectors\ of\ values\ V, and\ another\ of\ LocalMaximums_{indexes}\ (LM_{indexes}):$$

$$Boolean\ vector\ B(n) = \begin{cases} 1, if\ V(n) > V\big(LM_{indexes}(k)\big) - dB\ Limit \\ 0, if\ V(n) \leq V\big(LM_{indexes}(k)\big) - \ dB\ Limit \end{cases}$$

We define the Section of 1's where our local maximum is located (Explained later):

$$Section\ S\ is\ defined\ as\ a\ vector\ of\ indexes$$

$$Maximum\ of\ a\ lobe = \begin{cases} 1, true\ if\ max\big(V(S)\big) = V\big(LM_{indexes}(k)\big) \\ 0, false\ if\ max\big(V(S)\big) \neq V\big(LM_{indexes}(k)\big) \end{cases}$$

$$Each\ step\ for\ k = 1,2,3\ldots K = number\ of\ Local\ Maximums\ in\ V$$

```
function [is_lobe_maximum]= isLobeMax(magnitude, maximum_candidates, margin)

num_candidates=length(maximum_candidates);
is_lobe_maximum=false(num_candidates,1);
 for i=1:num_candidates

    boolean_overmargin=magnitude>magnitude(maximum_candidates(i))-margin;

    section_indices=takeSection(maximum_candidates(i), boolean_overmargin);
```

```
        if magnitude(maximum_candidates(i))== max(magnitude(section_indices))

            is_lobe_maximum(i)=true;
        else
            is_lobe_maximum(i)=false;
        end
   end
```

To take the Section that belongs to the lobe of the local maximum (our candidate) it is necessary to perform some other operations. For example, let's define:

A=[0, 0, 1, 1, 1, 0, 0, 0, 1, 1, 1, 1] How can we take the first section of 1's: $A(a_3\ to\ a_6)$?

*In a general case, given a boolean vector B and the index of local máximum **m**:*

$$B_{mod} = [b_2, b_3, b_4, \dots, b_n, \dots b_N, b_1]$$

$$Substraction\ S = B_{mod} - B$$

$$S = \begin{cases} 1, & if\ it's\ the\ beginning\ of\ a\ section\ 1's \\ -1, & if\ it's\ the\ end\ of\ a\ section\ of\ 1's \\ 0, & it's\ not\ a\ part\ of\ a\ section\ of\ 1's \end{cases}$$

*Start Section = n index value when we take the last $S(n) = 1$ and $n < m$*

*End Section = n index value when we take the first $S(n) = -1$ and $n > m$*

*Section = [Start Section, Start Section + 1, Start Section + 2, …. End Section]*

```
function [section_indices]=takeSection(maximum_candidate, boolean_overmargin)

boolean_overmargin_new=[boolean_overmargin; boolean_overmargin(1)];
change= diff(boolean_overmargin_new);

index_increase=find(change==1);
index_decrease=find(change==-1);

start_section=find(index_increase<maximum_candidate(1), 1, 'last');
end_section=find(index_decrease>maximum_candidate(1), 1, 'first');

section_indices=index_increase(start_section):index_decrease(end_section);
end
```

At this point, we have already all the indexes of local maximums and a boolean vector that say as which of that local maximums are a maximum of a lobe. To filter just the useful results:

$$Maximums\ of\ lobes_{indexes} = Local\ Maximums_{indexes}(Maximums\ of\ a\ lobe)$$

*Let's define number of lobes as **L** (length of vector Maximums of lobes$_{indexes}$)*

*And $Lobe_{matrix}$ as the result we want with dimensions $Lx5$ where:*

*Each Row is a different Lobe*

$Column\ 1 =\ Beamwidth\ of\ the\ lobe$

$Column\ 2 =\ Start\ Angle\ of\ the\ lobe$

$Column\ 3 =\ End\ Angle\ of\ the\ lobe$

$Column\ 4 = Main\ direction\ of\ the\ lobe = Theta_{\pi/rad}(Maximum\ of\ lobes_{indexes}(l))$

$Column\ 5 = dBi\ level\ on\ main\ direction\ of\ the\ lobe = V\big(Maximum\ of\ lobes_{indexes}(l)\big)$

*All these steps for $l = 1, 2, ... L$*

```
lobe_maximums=local_maximums(is_lobe_maximum);
number_lobes=length(lobe_maximums);
lobes=zeros(number_lobes, 5);

for i=1:number_lobes
beamwidth=findBeamwidth(T.Abs, theta_rad_360, lobe_maximums(i), dB_limit);
main_direction=theta_rad_360(lobe_maximums(i));
dBi_level=T.Abs(lobe_maximums(i));
lobes(i, :)=[beamwidth, main_direction, dBi_level];

end
```

| 4x5 double | | | | |
|---|---|---|---|---|
| 1 | 2 | 3 | 4 | 5 |
| 0.2722 | 0.1556 | 0.4278 | 0.2722 | 5.9060 |
| 0.2722 | 0.5667 | 0.8389 | 0.7278 | 5.9060 |
| 0.1167 | 1.2500 | 1.3667 | 1.3111 | 2.5420 |
| 0.1167 | 1.6278 | 1.7444 | 1.6889 | 2.5420 |

The Columns 1, 2 and 3 have been calculated with another function:

*Given dB Limit, vectors $V$ and $Theta_{\pi/rad}$ and index $m$ (maximum of a lobe)*

*Again we generate a boolean vector $B(n)$ where $b_n$ is true if $V(n) > V(m) - dB\ Limit$*

Then, we take the Section of 1's where V(m) belongs (explained in previous steps).

$Angles_{section} = Theta_{\pi/rad}(Section)$

$$Column\ 2 = Cutoffangle_1 = Angles_{section}(1)$$
$$Columns\ 3 = Cutoffangle_2 = Angles_{section}(end)$$
$$Column\ 1 = Cutoffangle_2 - Cutoffangle_1$$

```
function [beamwidth_long]=findBeamwidth(magnitude, angles, lobe_maximum, margin)

boolean_maximum_sections=magnitude>magnitude(lobe_maximum)-margin;
beamwidth index=takeSection(lobe maximum, boolean maximum sections);
one_section=angles(beamwidth_index);

cutoff_angle1=one_section(1);
cutoff_angle2=one_section(end);
beamwidth = cutoff angle2-cutoff angle1;

beamwidth_long=[beamwidth, cutoff_angle1, cutoff_angle2];

end
```
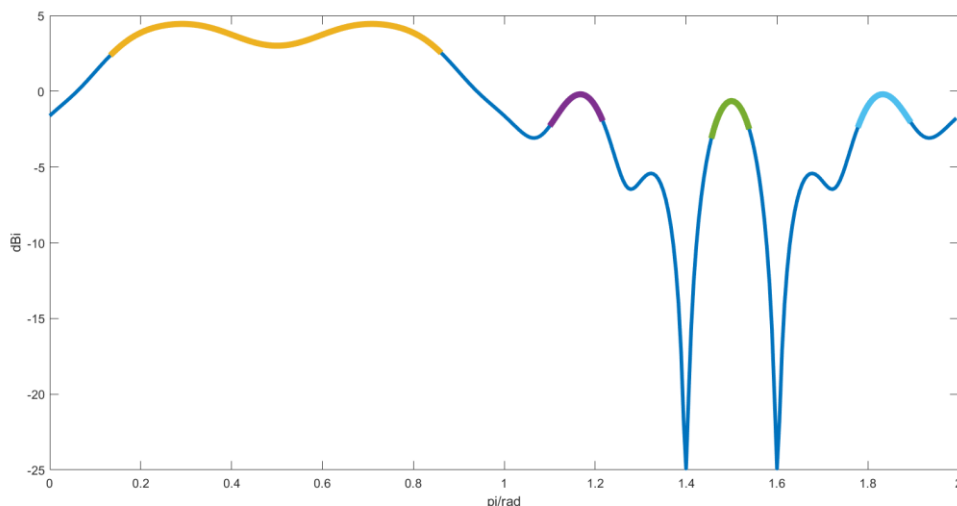
Finally to plot all the results of the Radiation Pattern:

```
plot(theta_rad_360, T.Abs)
xlabel('pi/rad')
ylabel('dBi')
hold on

for n=1:number_lobes
plot(theta_rad_360(find(theta_rad_360==lobes(n, 2)):find(theta_rad_360==lobes(n, 3))),
T.Abs(find(theta_rad_360==lobes(n, 2)):find(theta_rad_360==lobes(n, 3))))
hold on
end
```



### Volumes and sizes

At this point we will try to see how we have calculated the different encapsulations of the antenna. To do this, we have made use of Matlab and have established some rules to scale the volumes.

Most of the encapsulations are cylindrical and their volume corresponds to the formula:

$$V_{cylinder}(r, l) = \pi r^2 l$$

To scale this volume to $nV_1(r_1, l_1)$ it is necessary to establish an arbitrary relationship between r and l. That relationship is k=l/r, which means that l=kr. Knowing the original volume (V1) and how big we want to make it (n), we can know the final volume $V_2 = nV_1$. So, we can derive the new radius and length of the new cylinder keeping the constant k:

$$V_2(r_2, l_2) = nV_1(r_1, l_1) = \pi r_2^2 l_2 = \pi r_2^2 k r_2$$

$$r_2 = \sqrt[3]{\frac{V_2}{\pi k}} \; ; l_2 = kr_2$$

However, it may be that this constant k cannot be kept constant if the new l is less than the length of the antenna $\lambda/4$, which in our case is 30.61 mm at 2.45 GHz. Therefore, this measure has been left as the minimum length, leaving a small margin of 1 millimeter.

$$if\,(using\;last\;method)\;l_2 < \lambda/4, then\;l_2 = \lambda/4 + 1$$

$$and\;r_2 = \sqrt[2]{\frac{V_2}{\pi l_2}}$$

```
function [length_new_cyl, radius_new_cyl]= ScaleCylinder(length_cyl, radius_cyl, scale)

lambda_4=30.6122;

volume=cylinder_volume(length_cyl, radius_cyl);
new_volume=scale*volume;
k=length_cyl/radius_cyl;
length_cyl_2=k*radius_cyl;
aux=new_volume/(pi*k);
radius_new_cyl=nthroot(aux, 3);
length_new_cyl=k*radius_new_cyl;

if length_new_cyl<lambda_4+1

    length_new_cyl=lambda_4+1;
    radius_new_cyl=sqrt(new_volume/(pi*length_new_cyl));
end
end
```

On the other hand, when we want to model a pill shape (composed of a cylinder and two hemispheres at each end of the cylinder), we have calculated its volume as follows:

$$V_{pill}(r_{pill}, l_{pill}) = V_{cyl}(r_{cyl}, l_{cyl}) + 2V_{hemisphere}(r_{sph}) = V_{cyl} + V_{sphere}$$

$$where\;r_{pill} = r_{cyl} = r_{sph}, \quad and\;l_{cyl} = l_{pill} - 2\,r_{sph}$$

$$V_{sphere} = \frac{4\pi r^3}{3}$$

The default "cylinder" and "sphere" functions in Matlab are generated with 21 reference points. Therefore, in the case of spheres, we take only half of the values ([1:11] or [11:21]) to make them hemispheres. When we use the surf command, we are positioning the origin of the spheres, that is, their center, oriented on the z axis at a height of l/2 and -l/2 respectively.

```
function [volume, length_equivalent_cylinder]=pillvolume(total_length, radius)

length_cylinder=total_length-2*radius;
volume_cylinder_pill=pi*radius^2.*length_cylinder;
volume_sphere=4/3*pi*radius^3;

volume=volume_cylinder_pill+volume_sphere;
length_equivalent_cylinder=lengthCylin(volume, radius);
```
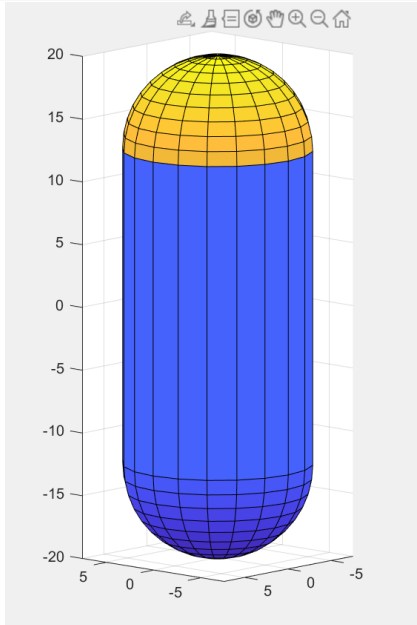


```
[x, y, z]=sphere;
l=length_cylinder;
r= radius;
%sphere1
x2=x(11:21,:)*r;
y2=y(11:21,:)*r;
z2=z(11:21,:)*r;
surf(x2,y2,z2+l/2)
axis equal
hold on
%sphere2
x5=x(1:11,:)*r;
y5=y(1:11,:)*r;
z5=z(1:11,:)*r;
surf(x5,y5,z5-l/2)
%cylinder
[x3,y3,z3]=cylinder;
x4=x3*r;
y4=y3*r;
z4=z3*l;
surf(x4,y4,z4-l/2)
end
```

To convert a cylinder with a given volume to a pill shape model with the same volume, three criteria can be used: maintain the k ratio, mentioned before, and therefore the radius/length ratio, the second option would be to maintain the radius r and vary only the length, which is desirable if the same thickness of human tissue is to be passed through; thirdly, the length l can be kept constant, but this criterion does not offer any advantage (neither does it maintain the ratio, nor does the wave pass through the same amount of tissue).

For the first criterion we will make use of some definitions already mentioned:

$$given\ this\ desired\ volume\ V_{cyl}(r_{cyl}, l_{cyl})\ and\ k\ defined\ as\ l/r$$

$$Due\ to\ l_{total,pill} - 2\,r_{pill} = kr - 2r = r(k-2)$$

$$V_{cyl} = V_{pill} = r^3\pi(k-2) + 4\pi r^3/3 = r^3\pi\big((k-2) + 4/3\big)$$

$$r_{pill} = \sqrt[3]{\frac{V_{pill}}{\pi\big((k-2)+4/3\big)}}$$

With the second criterion, maintaining the same radius as the cylinder we want to convert:

$$r_{cyl} = r_{pill}; \qquad V_{cyl} = V_{pill}$$

$$l_{pill} = \frac{V_{pill} - \frac{4\pi r^3}{3}}{\pi r^2}$$

**Representation of efficiencies**

The radiation efficiencies provided by the CST can be plotted in a simple way. It is possible to reorder the efficiencies in a single matrix to represent them all at once by one function.

$$Given\ a\ matrix\ of\ efficiencies\ E_{rxc},$$

$$where\ R\ (rows)\ reprents\ the\ different\ simulations\ and\ C\ (columns)\ each\ position\ point$$

$$And\ given\ a\ Step(mm)\ we\ can\ create\ vector\ D\ that\ represents\ the\ distance\ axis$$

$$d_n = (n-1)\cdot Step, \qquad from = 1,2,3,\dots to\ C$$

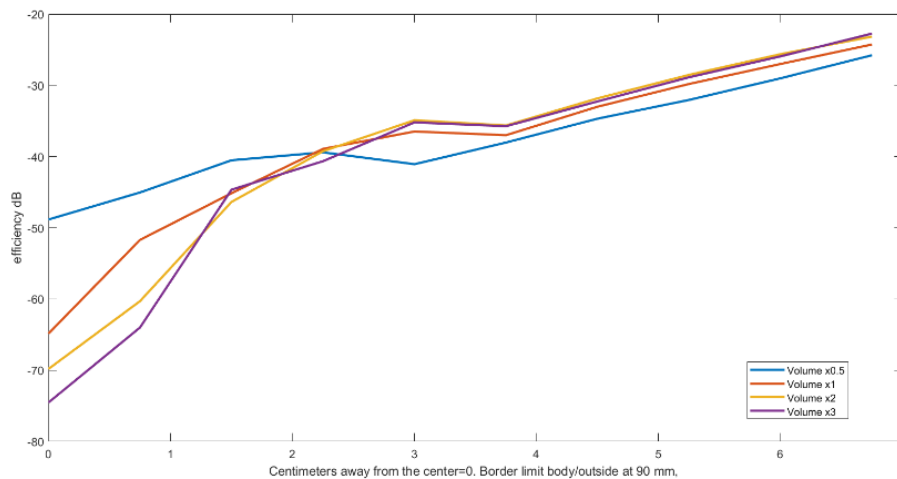$$At\ the\ end, we\ have\ to\ plot\ d_n\ (x-axis)\ and\ E(r,c)\ (y-axis)$$

$$for\ each\ r = 1,2,\dots to\ R$$

```
function []=plot_effic(Eff_matrix, step)
[r1,c1]=size(Ef_matrix);

centimeters=zeros(1,c1);

for i=1:1:c1
    centimeters(i)=i*step-step;
end

for i=1:r1
plot(centimeters(1,:), Ef_matrix(i, :), 'Linewidth',2);
hold on
end
```



Because we have not performed simulations at every point, we can use *fit* function in matlab tool to approximate our samples to a polynomial function.

$$f_n(x) = p_1 \cdot x^n + p_2 \cdot x^{(n-1)} \dots p_n \cdot x + p_{n+1}$$

```
f3 = fit(centimeters', Ef_matrix(1,:)', 'poly3')
y_teorical_3 = f3(centimeters)
```

```
                Linear model Poly3:
                f3(x) = p1*x^3 + p2*x^2 + p3*x + p4
                Coefficients (with 95% confidence bounds):
                  p1 =        0.122  (-0.02741, 0.2714)
                  p2 =       -1.131  (-2.668, 0.4058)
                  p3 =        5.526  (1.211, 9.841)
                  p4 =       -48.38  (-51.56, -45.2)
```
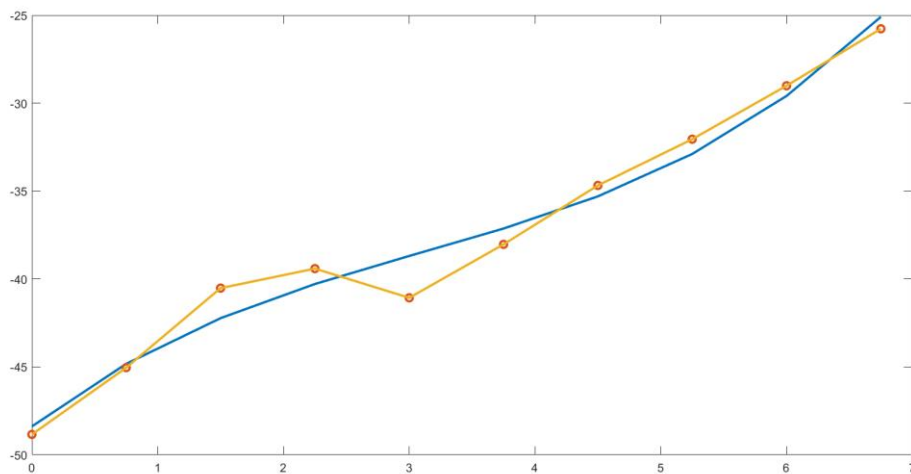


In the same way, we can make an approximation, not only of an encapsulation, but of all that we have done. It's to make a polynomial approximation of all the samples we have. But that's not really accurate.

As the points differ more, one can assume to increase the degree of the polynomial. However, in problems with many points, increasing the degree of polynomial adjustment does not always result in a better result. Higher order polynomials can oscillate between data points, leading to a worse adjustment to the data. In those cases, a lower order polynomial adjustment or a different technique can be used, depending on the problem.

In other words. A setting with a very high polynomial order can very well adjust a few samples to a function but only in a particular section. The problem is this: it is over-adjusted.

When you try to estimate another new sample with the approximate function, the result will be quite inaccurate. If it is over-adjusted at all points, it is over-adjusting the noise too.This is not convenient, as it does not show reality because we are treating the noise as part of the model and not as undesirable noise.

# Chapter 5: Performance of lambda quarter planar antenna

It has been possible to physically build the quarter lambda antenna designed in CST . When taking simulation designs to reality, there will always be differences from the simulations in the results. This is due to the imperfections that we do not find in the CST because: the simulated materials are perfect electrical conductors (PEC), in the simulation the symmetries and forms are ideal, the simulated measures with computational processes do not induce so many errors in the measures.

However, in reality materials have losses, regularity in shapes and perfect symmetries do not exist and there can always be errors in measurements due to mechanical failures, interference or electronic errors. It must be taken into account that with small antennas (in absolute terms) any minimum change (in millimetric scale) can mismatch the ideal data that we would like to achieve.
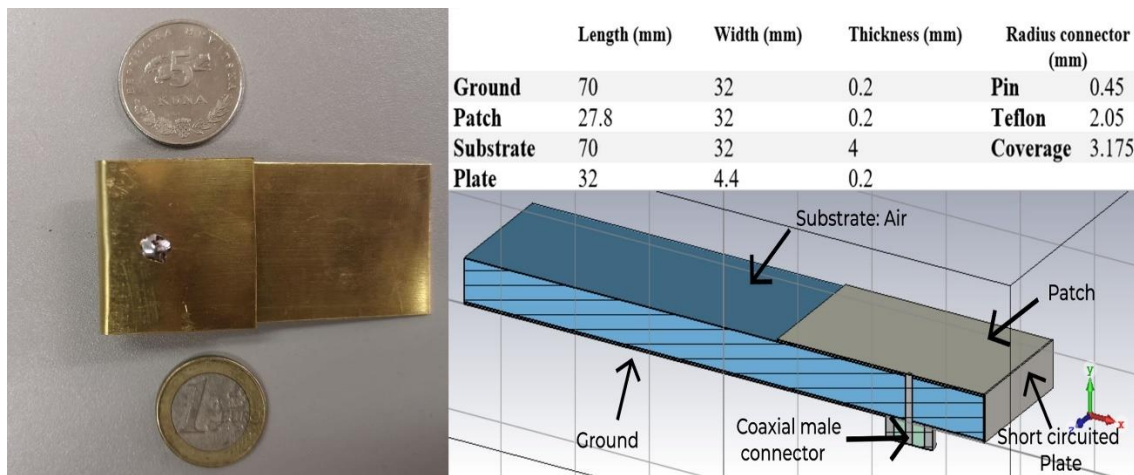
|  | Length (mm) | Width (mm) | Thickness (mm) | Radius connector (mm) | |
|---|---|---|---|---|---|
| Ground | 70 | 32 | 0.2 | Pin | 0.45 |
| Patch | 27.8 | 32 | 0.2 | Teflon | 2.05 |
| Substrate | 70 | 32 | 4 | Coverage | 3.175 |
| Plate | 32 | 4.4 | 0.2 | | |

**Figure 35-Antenna physically designed, coin as a scale (left). Sizes and CST design (right).**

With the network analyser it has been possible to analyse the performance of the antenna in those aspects related to the electrical properties such as the scattering parameters. The network analyser must be calibrated to take into account reference values. In addition, the losses introduced by the coaxial cables and connectors must be taken into account. In the following image it can be seen how the losses, as a function of the frequency, affect the range from 10 MHz to 40 GHz.
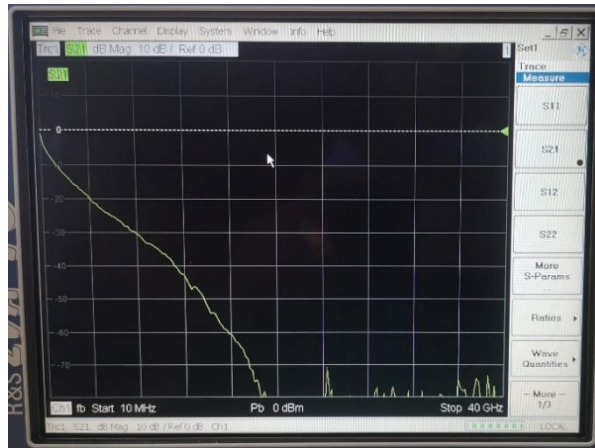
**Figure 36-Losses due to coaxial cables and connectors from 10 MHz to 40 GHz**

In this image we can see the same as in the previous figure but expanded, focusing on the range between 2 and 3 GHz. The marker is centered on the 2.45 GHz at which the antenna works. As you can see, before the calibration the cable losses are about 15dB and after the calibration they are no longer represented. Although they still exist, it is calibrated to not take them into account, as we are not interested in our measurements.
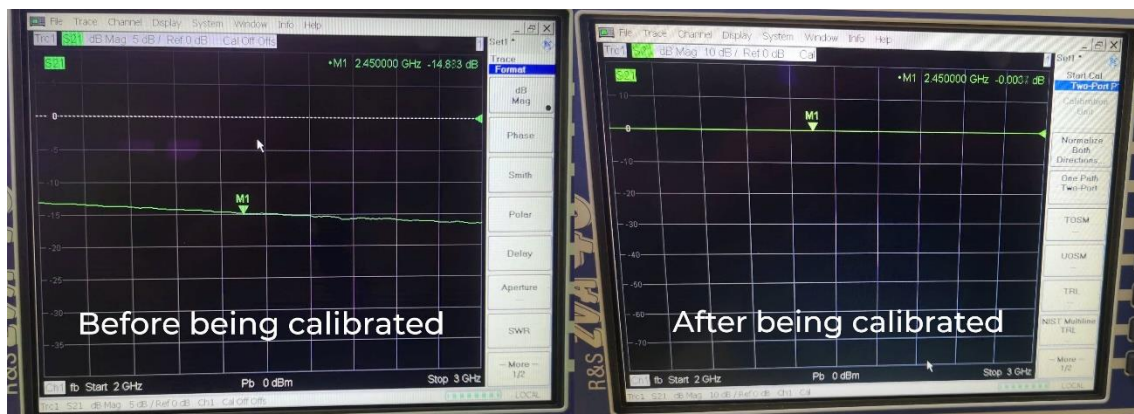


**Figure 37-Losses due to cables in the range of 2-3GHz befor and after calibration**

The antenna has been placed in the center of a modular anechoic chamber at a height of 1.26 meters and the receiving antenna has the same height. They both are separatedat horizontal distance of 1.57 meters. For field measurements, both antennas must be in direct line of sight, coinciding at their maximum points of transmission and reception (same height and directly facing). In addition, because we want to measure the far field, it is necessary to keep the antennas at a distance where we ensure that we are not measuring the near field.
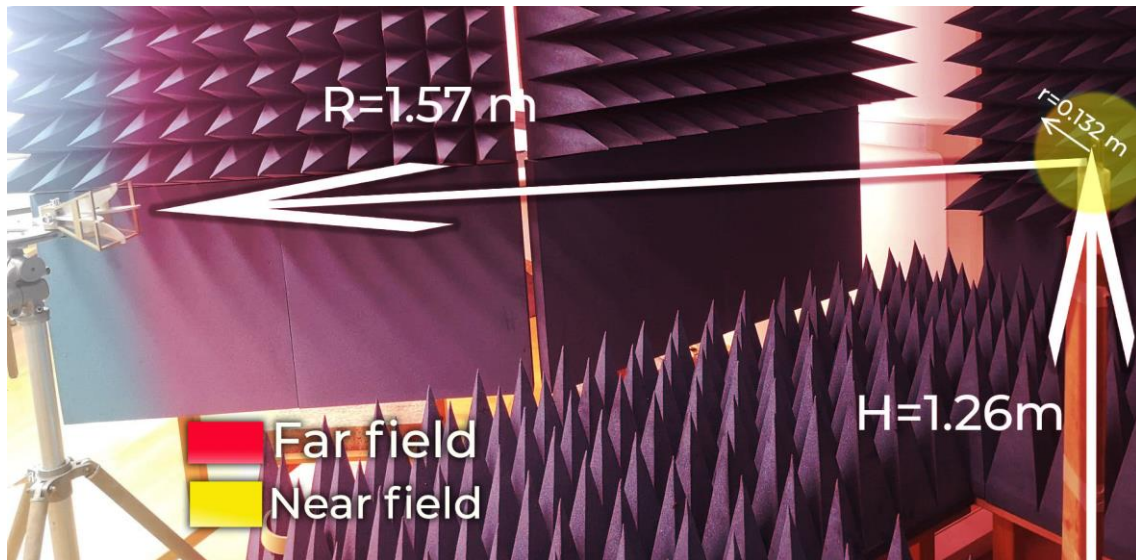
**Figure 38-Transmitting and receiving antenna placement**

In order to measure the radiation pattern, the plane of the electric field (E-plane) and the magnetic field (H-Field), we had to perform different measurements with the antennas correctly oriented. Taking the same axis references and establishing a correct reference angle (180 degrees maximum value), the results have been compared with those of the CST simulation.
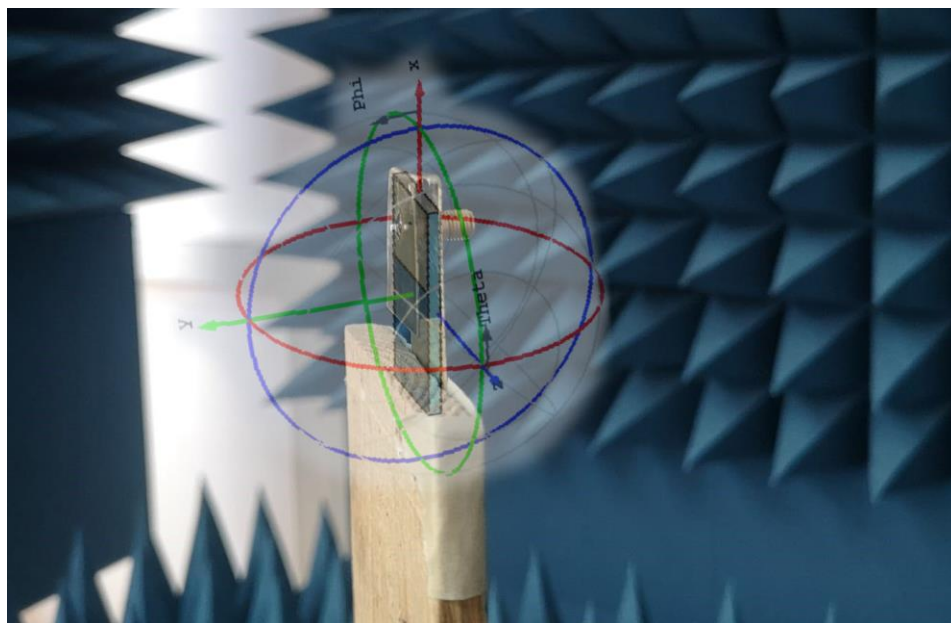


**Figure 39-Axis orientation of the antenna, measuring H plane (vertical position).**

For H-plane:

Vertical position
Y-axis: points the receiver.
X-axis: rotation axis, height from 0 to 360 degrees.
Z-axis: width of the antenna.

That's how we measure the ZY plane (Cartesian coordinates). This in CST is a perspective of radiation pattern with constant Phi=90 and Theta rotating from 0 to 180
and constant Phi=270 and Theta rotating from 180 to 0 (Polar coordinates).

For E-plane:

Horizontal position.
Y-axis: pointing the receiver.
X-axis: length of the antenna.
Z-axis: rotation axis, height from 0 to 360 degrees.

And the plane we were measuring is XY (Cartesian plane). This in CST is a perspective of radiation pattern with constant Theta at 90 degrees and phi from 0 to 360 degrees (Polar coordinates).

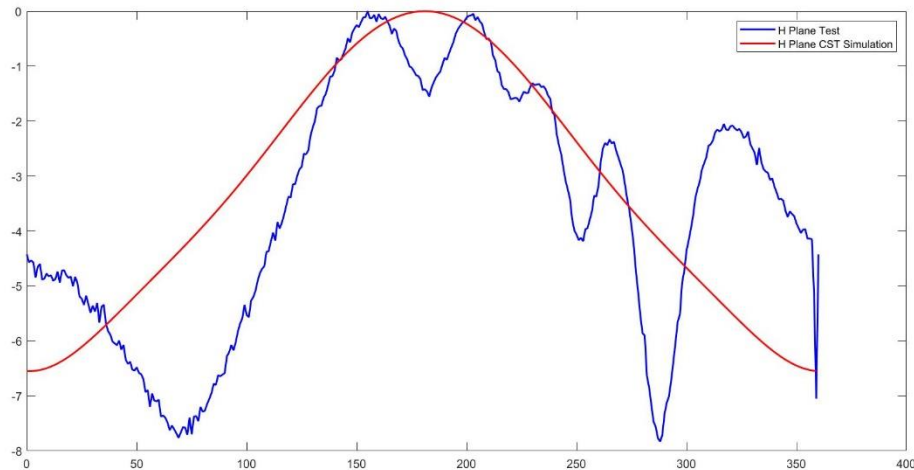In the following image we can see how the H-plane is represented both in CST and in the laboratory test.



**Figure 40-H-plane, radiation pattern 2D**

As we can see, there is a symetry in the H-plane of the CST because the antenna structure is symmetrical for those measurements. However, as we already advanced at the beginning of this topic, the performances are not perfect and in this case we found many drops due to interferences. This can be due to interference from the electric field as well as imperfections in the physical measurements, such as the imperfect shape or the cables themselves that can function as an antenna as well. With such small antennas, the size of the cables and the destructive interference they can add are quite relevant.

Measurement errors are common and not ideal like mathematical results. For example, we also observe a clearly erroneous value at angle 359, which presents an abrupt drop. As is done in statistical studies, this type of erroneous data can be discarded from the sample. Alternatives to this are the repetition of the measurements or an interpolation between adjacent data to continue the trend.
In the E-plane, we see how the shape of the radiation pattern is much more accurate. However, we observe how the lab results seem to be phase shifted to the left.This may be

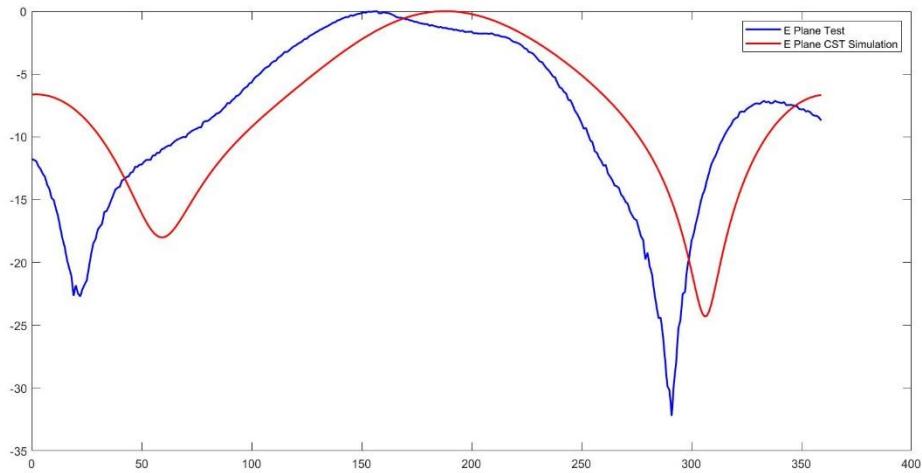due to a small mechanical error in orientation. Small millimeter changes can disturb the results.



**Figure 41- E-plane, radiation pattern 2D**

A logical change could be to align the maximum of the laboratory measurements with the maximum of the CST result measurements. This way we can center both graphs and compare them                                                                                                      better.
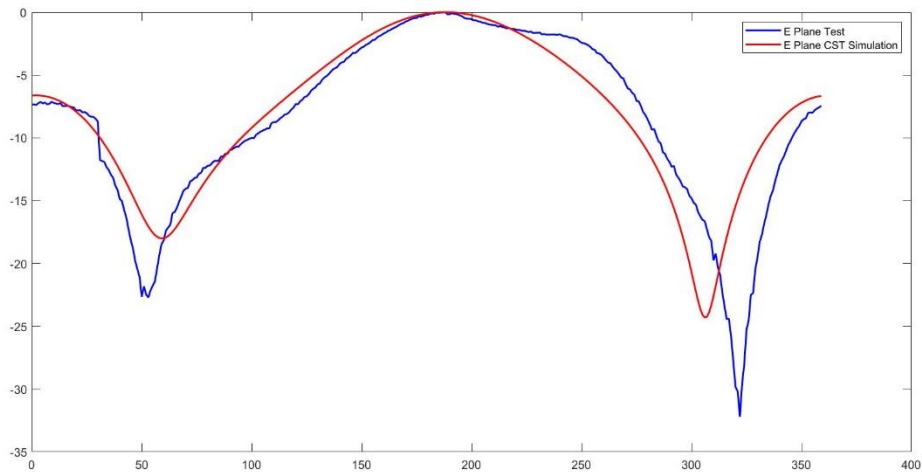


**Figure 42- E-plane, radiation pattern 2D, centered**

In the test results, we see two nulls in radiation pattern deeper than those of the CST. We also see that the main lobe is wider than the one simulated in the computer. In addition, some small peaks are added that make the graph less smooth locally due to totally normal imperfections. In general we can say that it has a good similarity to what was initially designed.

As we see in the image of the circuit, for the transmission lines to affect us the less, because it is very long in terms of lambda, Za must be equal to Z0. The impedance of the antenna is going to have a resistive part and a reactive part. Because the line has a characteristic resistive impedance, it is convenient that Za is also only resistive and not reactive: 50 ohms.

If Za=Z0, then Zin=Z0 regardless of the length of the line, that is when we say it is matched. If, in addition, Zin=Zs (resistivity of the source or generator), the maximum power transfer theorem will be satisfied.
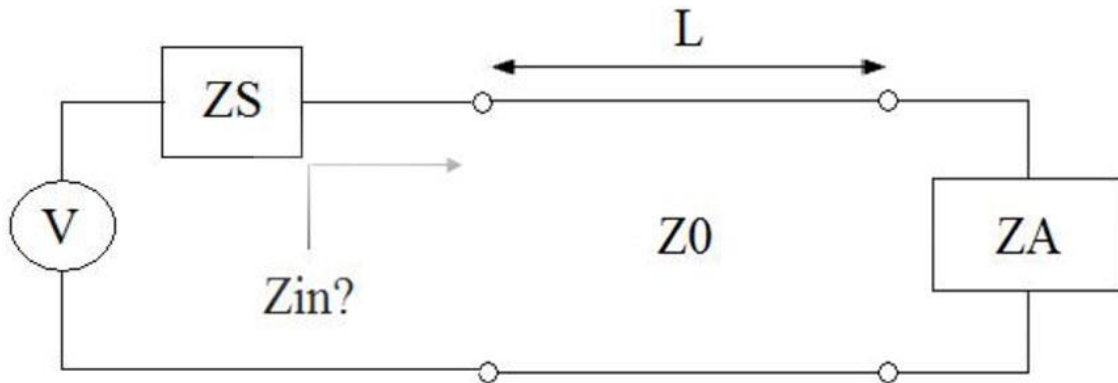


**Figure 43- Circuit schematic of transmissión line**

Here we can see Za's module as a function of frequency. At the frequency of 2.45 GHz in the CST the module of Za is 63.23 and in the laboratory it is 45.38 ohms.
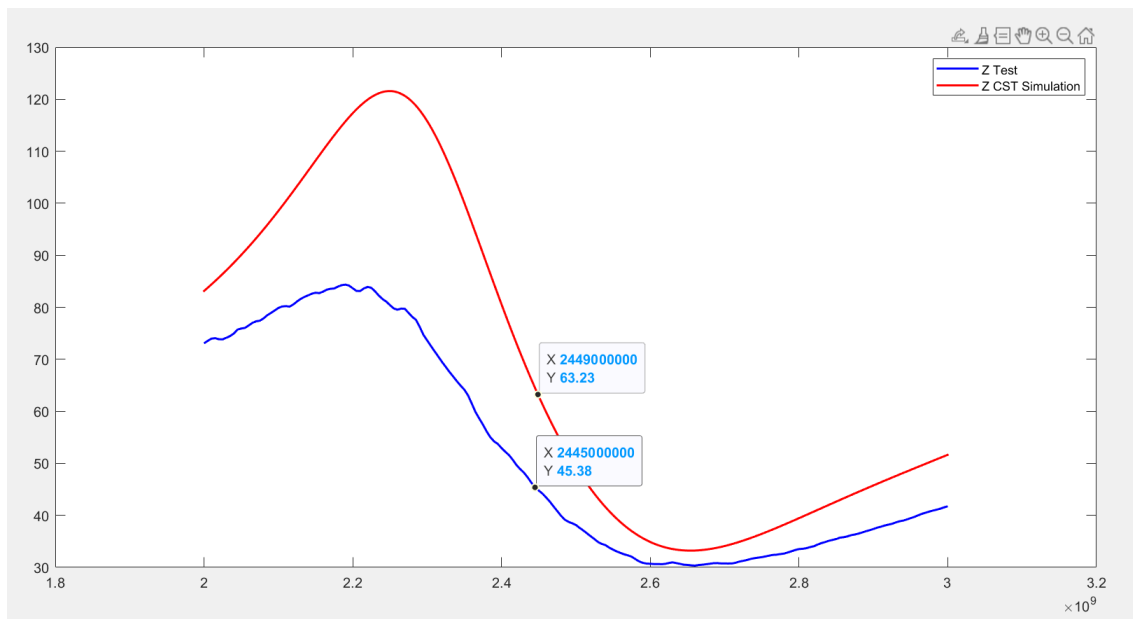


**Figure 44- Module of Antenna impedance**

In this other graph we can see the decomposition of the impedance of the antenna in its real (resistive) and imaginary (reactive) part. Ideally, the curve of the imaginary would be zero at 2.45 GHz. In the CST the imaginary part is worth 10.74 and in the laboratory 14.07 ohms.
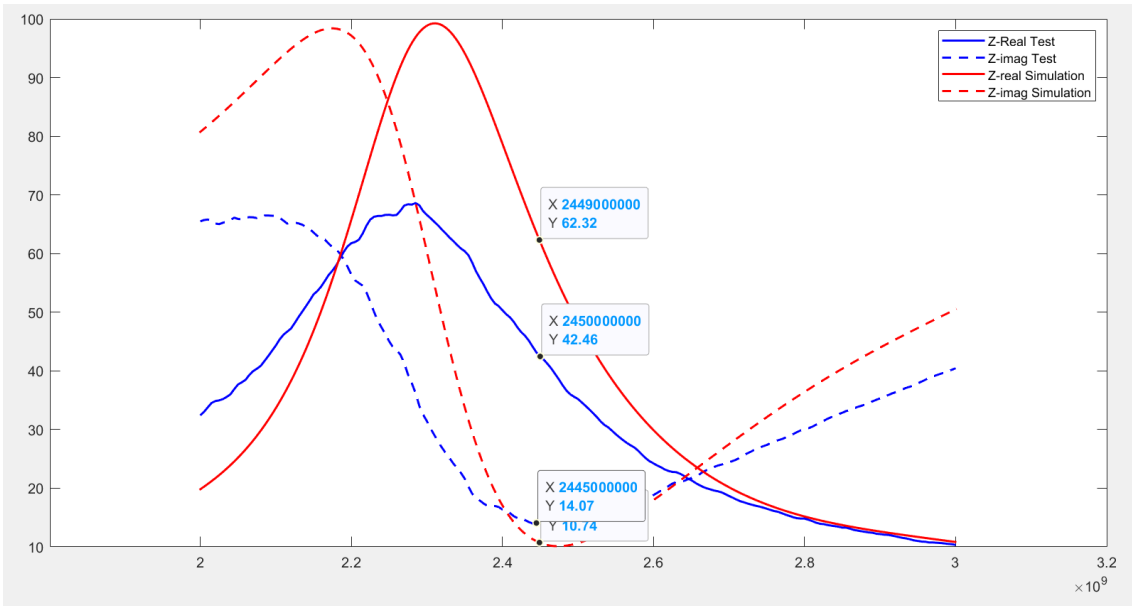
**Figure 45- Antenna impedance, real and imaginary part**

But even if the results of the antenna impedance are not ideal nor those simulated in CST we observe that in the end the antenna works. The reflection parameter s11, defined by the impedances of the antenna and the characteristic impedance of the line, reaches -15 dB for the frequency of 2.45 GHz, which we can consider an acceptable operation. Seeing the differences obtained with the simulation, we observe that in the simulation we reached -24 dB for 2.45 GHz and this was the deepest peak of the valley. In the case of the laboratory tests, the central working frequency is shifted to lower frequencies, close to 2.4 GHz. However, the bandwidth is wide enough to reach 2.45 GHz and still function properly.
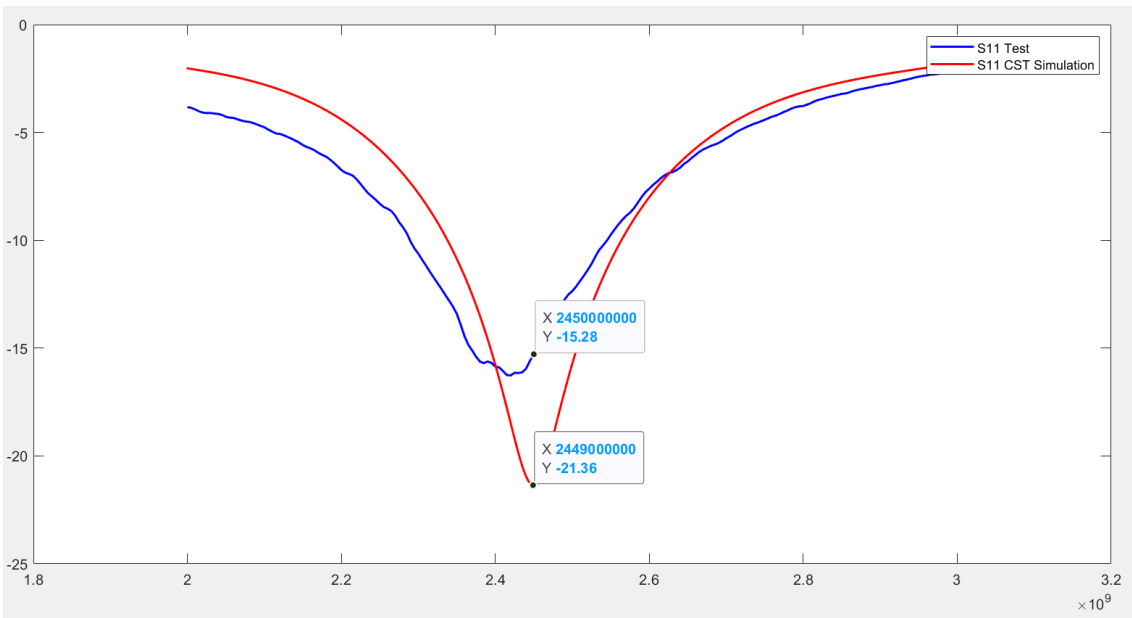


**Figure 46- S11 parameter**

# Conclusion

In this thesis we have been able to understand and have a wide general idea about biomedical implants. The need to equip them with an antenna is becoming more and more necessary for medical monitoring and has, without a doubt, a place in the medicine of tomorrow. We have been able to simulate different scenarios where the human body has been a clear obstacle to the efficiency of our antenna. On top of that, dealing with high absorption environments gives worse results when the antenna has to be also necessarily small, both physically and electrically.

Through the simulations we have proven what the theory tells us. The wireless link improves as we get closer to the surface and passes through less and less of the dielectric. However, not everything has been so obvious, each simulation, depending on the position and the encapsulation, has had its variations and differences. We have observed that the smaller volumes were more efficient for areas near the center of the body than the big ones, although in the final position (near the edge of the body) they were the less efficient.

Similarly, although efficiencies were improving when approaching the edge of the body, directivity behaves differently. This means that, although efficiency measures total radiated power, choosing to focus power in one direction may also be a better option even if some efficiency is reduced.

If we only look at the results of this project we could say that in the case of implanting an antenna, the best result would be given with a encapsulation as large as possible, within the medical guidelines, and located far from the center of the body, avoiding symmetry in the radiation.

But the reality is that in the human body symmetry is avoided in practically all cases, even in the geometric center, due to the heterogeneity of the tissues. Furthermore, to characterize these results as a polynomial would be somewhat uncertain. Small changes in the parameters in the small antennas and the simulations can cause big variations in the model, so a large number of simulations would be needed and to establish a robust model in collaboration with the entire research community specializing in this.

To handle all these dozens of simulations and data we have learned how to deal with them using Matlab codes. These codes have essentially been an analysis of data from discrete samples. It has been possible to make useful and practical use of data vectors for its representation and detection of relevant data in the discrete functions as well as it has served us as a tool to scale the volumes under a criterion.

In spite of everything, and being the implants a research path with a lot to do, the thesis work has a lot of potential for improvement. Simulations with heterogeneous bodies that simulate different tissues, other encapsulation geometries or a practical test with phantoms, which we hope to perform in the future, are some of them. Nevertheless, biomedical implants have many challenges, especially the one related to wireless communications which will hopefully be an area of research with good results in the coming years.

# References

*[1] Antenna Designs for Wireless Medical Implants, Conor P. Conran, 2013, Dublin Institute of technology*

*[2] Antennas and Propagation for Body-Centric Wireless Communication, Peter S. Hall Yang Hao, 2006 ARTECH HOUSE, INC. 685 Canton Street Norwood, MA 02062*

*[3] A Review of In-Body Biotelemetry Devices: Implantables, Ingestibles, and Injectables*

*Asimina Kiourti, Member, IEEE, Konstantina S. Nikita, Senior Member, IEEE Transaction on Biomedical Engineering July 2017 First published as a Review in Advance on February 28, 2018*

*[4] Wearable and Implantable Sensors for Biomedical Applications, Hatice Ceylan Koydemir and Aydogan Ozcan, Annu Rev Anal Chem (Palo Alto Calif) 2018 Jun*

*[il.1] Connectingin-Body nano communication with body area networks:Challenges and opportunities of the Internet of Nano Things, Falco Dressler, Stefan Fischer, Elsevier, 2015  Nano Communication Networks, Volume 6, Issue 2, Pages 29-38.*

*[5] An integrated low-power Binary-PAM based wireless telemetry circuit for implantable cardiac pacemakers Jiangtao Xu, Yujian Zhai, Yang Yang , Ruizhi Zhang , Hong Zhang, Elsevier, Microelectronics Journal, Volume 99, May 2020*

*[6] The Biomedical Engineering Handbook, Third Edition, Medical Devices and Systems, edited by J.Bronzino, Chapter 54, Taylor&Francis, 2006*

*[7] Psychoacoustics, Facts and Models. E. Zwicker. H. Fastl., Facts and Models, 2007.*

*[8] J. Weber: Medical Instrumentation, Chapter 13, Cochlear Prosthesis*

*[9] Leadless Dual-Chamber Pacing A Novel Communication Method for Wireless Pacemaker Synchronization Lukas Bereuter, MSC, a,b Mirco Gysin, MSC, b Thomas Kueffer, MSC, a,b Martin Kucera, MSC, c Thomas Niederhauser, PHD,c Jürg Fuhrer, MD,a Paul Heinisch, MD,d Adrian Zurbuchen, PHD,e Dominik Obrist, PHD,b Hildegard Tanner, MD,a Andreas Haeberlin, MD, PHDa,b, Elsevier, JACC: Basic to Translational Science, Volume 3, Issue 6, December 2018, Pages 813-823*

*[10] Subretinal electronic chips allow blind patients to read letters and combine them to words Eberhart Zrenner, Karl Ulrich Bartz-Schmidt1, Heval Benav, Dorothea Besch, Anna Bruckmann1, Veit-Peter Gabel, Florian Gekeler1, Udo Greppmaier, Alex Harscher, Steffen Kibbel, Johannes Koch1, Akos Kusnyerik, Tobias Peters, Katarina Stingl , Helmut Sachs, Alfred Stett, Peter Szurman, Barbara Wilhelm and Robert Wilke1, Proc Biol Sci. 2011 May 22; 278(1711): 1489–1497.*

*[11] Sensors and Actuators A 130–131 (2006) 609–615Fabrication of pyramid shaped three-dimensional 8×8electrodes for artificial retinaKyo-in Koo, Hum Chung, Youngsuk Yu,Jongmo Seo, Jaehong Park, Jung-Min Lim,Seung-Joon Paik, Sungil Parka,c,d,e,f,g, Hyun Min Choi,Myoung-Jun Jeong, Gil Sub Kim, Dong-Il Dan Cho*

*[12] NINA-W10 series Stand-alone Multiradio modules Data sheet, ublox, Apr-2020*

*[13] EMI Protection for Communication Systems, Kresimir Malaric, Artech House, 2009*

*[14] Fundamentos de líneas de transmisión. Vicent M. Rodrigo, Vicente E. Boria, Pablo Soto, Universitat Politècnica de València, 2019*

*[15] Teoría de Antenas. Jaume Anguera y Antonio Pérez, Lluís Vicent, 2008*

*[16] Confundiendo al confuso: reflexiones sobre el factor de impacto, el índice h(irsch), el valor Q y otros cofactores que influyen en la felicidad del investigador Guillermo Quindós, Revista Iberoamericana de Micología, ISSN 1130-1406, Vol. 26, Nº. 2, 2009, págs. 97-102*

*[17] Detailed Modeling of the Human Body in Motion to Investigate the Electromagnetic Influence of Fields in a Realistic Environment. Dr.-Ing. Thomas Weiland, Prof. Dr.-Ing. Herbert De Gersem , Zur Erlangung des akademischen Grades Doktor-Ingenieur (Dr.-Ing.) genehmigte Dissertation von M.Sc. Marija Nikolovski geb. Vuchkovikj aus Skopje, Mazedonien Tag der Einreichung: 09.05.2017, Tag der Prüfung: 12.07.2017 Darmstadt 2018 — D 17*

*[18] Evaluating Compliance With FCC Guidelines for Human Exposure to Radiofrequency Electromagnetic Fields, 97–01 ed. Washington, DC: Federal Communication Commission (FCC) Std. Supplement C, OET Bulletin 65, p. 35, 2001*

# SUMMARY

Wearable or implantable devices are becoming very interesting for medical applications where remote monitoring of patients or their condition is required. These biomedical implants need to be designed according to medical guidelines and should not interfere with the patient's daily life. This limits some parameters of the implant design such as size, geometry, or available power among others. This thesis should give an overview of the technologies applicable to medical implants and their relationship with wireless communications, as well as check how these design restrictions work in their performance. Taking into account these restrictions, the available simulation tools have been used and an antenna and a wireless system have been designed for an implantable device capable of radiating over a 2.45 GHz link. The capacity of the link has been tested for different implantable scenarios in a simulated environment as well as guidelines and methods have been established for their realization and subsequent analysis of the data.